European Journal of Pharmacology 998 (2025) 177600

Contents lists available at ScienceDirect

European Journal of Pharmacology

journal homepage: www.elsevier.com/locate/ejphar

Pro-histaminergic drug restores balance, promotes microgliogenesis and modulates neuroinflammation after vestibular injury

Jessica Trico [a,f,1], Emna Marouane [a,b,f,1], Isabelle Watabe [a], Agnes Lapotre [a], Alain Tonetto [c], Andreas Zwergal [d,e], Christian Chabbert [a,f], Brahim Tighilet [a,f,*]

[a] Aix Marseille University, CNRS, CRPN (Centre de Recherche en Psychologie et Neurosciences - UMR 7077), Marseille, France
[b] Normandie Université, UNICAEN, INSERM, COMETE, CYCERON, CHU Caen, 14000, Caen, France
[c] Aix Marseille University, CNRS, Centrale Marseille, FSCM (FR 1739), PRATIM, F-13397 Marseille, France
[d] Department of Neurology, LMU University Hospital, Munich, Germany
[e] German Center for Vertigo and Balance Disorders, LMU University Hospital, Munich, Germany
[f] Groupe de Recherche Vertige (GDR 2074), CNRS, Marseille, France

ARTICLE INFO

Keywords:
Vestibular syndrome$_1$
histamine$_2$
Vestibular compensation$_3$
Rodent posturography
Reactive plasticity
Microglia

ABSTRACT

Vestibular compensation is a neurobiological process that allows the recovery of impaired vestibular functions after unilateral vestibular damage. Among the post-injury plasticity mechanisms expressed in the vestibular nuclei (VN) that promote the restoration of balance function, neurogliogenesis and excitability changes appear to be in the forefront. At the central level, the vestibular syndrome expression results from an electrophysiological imbalance between both VN, known to activate the central histaminergic system. In this study, we aimed to investigate the impact of pharmacological modulation of the central histaminergic system on balance function recovery and its underlying post-injury mechanisms in the deafferented VN. For this purpose, we used a histamine analog, betahistine dihydrochloride (BD), which increases histamine synthesis and release in the VN through its histamine H3 autoreceptor antagonistic properties. The effect of BD treatment was tested in 3 animal groups: a UVN BD group subjected to unilateral vestibular neurectomy (UVN) treated orally during 10 days (50 mg/kg/day), a UVN placebo group (control), and a SHAM group. We show for the first time, in a UVN rodent model, the effects of BD on the reduction of the vestibular syndrome and highlight new targets and impact of this drug at the cellular level. Indeed, the results show that treatment with BD significantly attenuates the number of astrocytes and microglia which are key components of neuroinflammation. BD also prioritizes the differentiation of neoformed cells towards a microglia phenotype. These results, which need to be confirmed and further investigated by identifying the histaminergic receptors responsible for this effect, may lead to new therapeutic targets in vestibular pathology.

1. Introduction

Unilateral vestibular system dysfunction causes asymmetry between the bilateral vestibular nuclei (VN) resulting in characteristic symptoms. Data from the literature support that restoring electrophysiological balance between the ipsilateral and contralateral VN is crucial for post-lesion recovery of postural, locomotor, and gaze stabilization functions (Lacour and Tighilet, 2010; Smith and Curthoys, 1988a, 1988b). This process of cellular and behavioral plasticity, known as vestibular compensation, occurs over time and involves various plasticity mechanisms within the deafferented VN (Dutheil et al., 2009, 2016; Marouane et al., 2021; Rastoldo et al., 2022).

Histamine (HA), synthesized by histaminergic neurons located in the tuberomammillary nuclei (TMN) of the posterior hypothalamus, is involved in vestibular compensation (Tighilet et al., 2006). The TMN is directly connected to the VN (Matsuyama et al., 1996) and detects the

Abbreviations: betahistine dihydrochloride, BD; bromodeoxyuridine, BrdU; histamine, HA; histamine receptor, HR; medial vestibular nuclei, MVN; tuberomammillary nuclei, TMN; type 1 histamine receptor, H1R; type 2 histamine receptor, H2R; type 3 histamine receptor, H3R; unilateral vestibular neurectomy, UVN; vestibular nuclei complex, VNC; vestibular nuclei, VN.

* Corresponding author.
E-mail address: brahim.tighilet@univ-amu.fr (B. Tighilet).

[1] Contributed equally to this study as co first-authors.

https://doi.org/10.1016/j.ejphar.2025.177600
Received 8 November 2024; Received in revised form 21 March 2025; Accepted 2 April 2025
Available online 7 April 2025

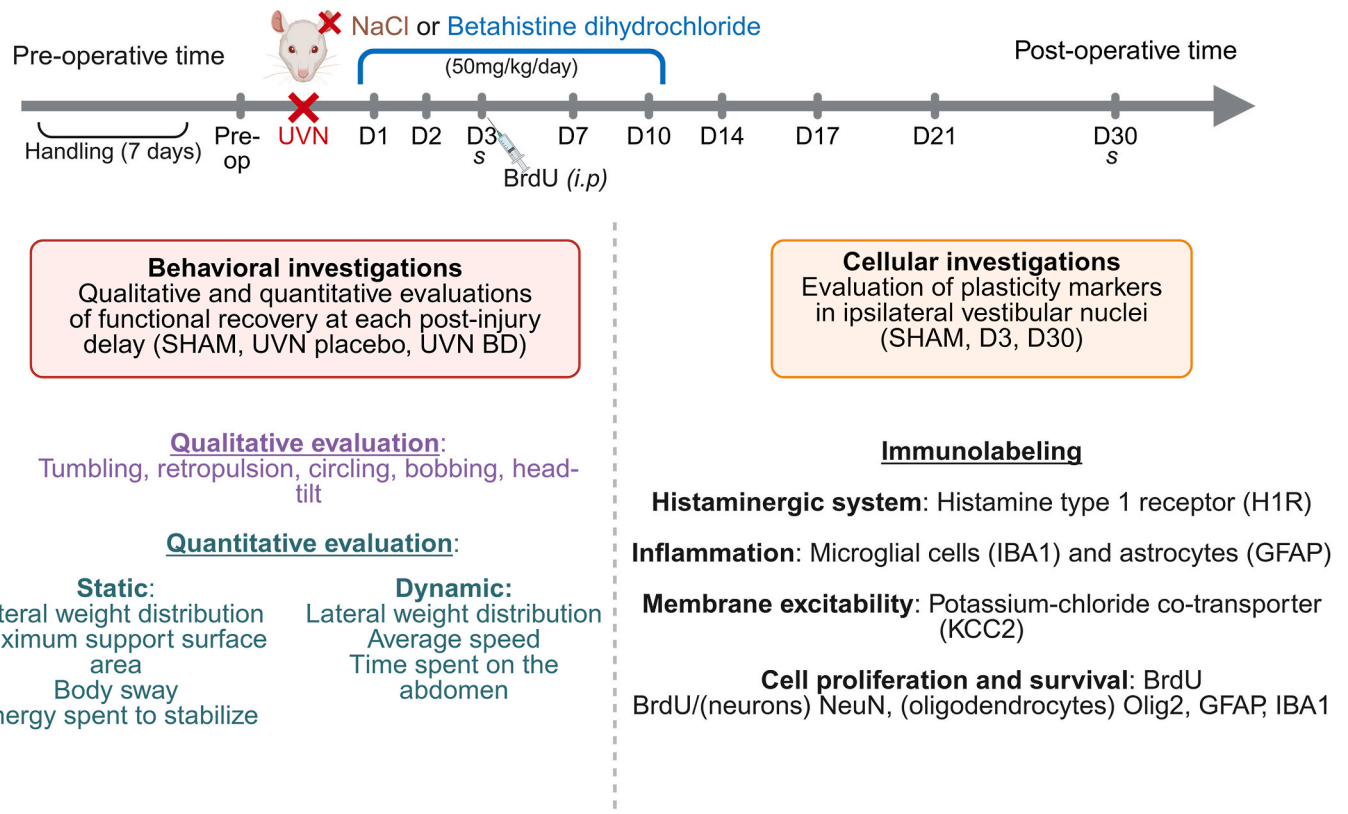

Fig. 1. Study design. Details of the procedures used to evaluate the impact of betahistine dihydrochloride treatment on the postural-locomotor components of vestibular syndrome and on the actors of vestibular plasticity. Behavioral investigations of the posturolocomotor component of the vestibular syndrome was made in a first preoperative session (serving as a reference value) and then at 1, 2, 3, 7, 10, 14, 17, 21 and 30 post-lesioned days for all the groups in the study (SHAM, UVN placebo and UVN BD). The treatments were administered (*per os*) to the animals daily from D1 to D10 post-UVN. Cellular investigations were performed at 3 and 30 days post-lesioned survival times. s: sacrifice, i. p; intraperitoneal injection.

electrophysiological imbalance between the VN, leading to increased synthesis and release of HA in the VN (Tighilet et al., 2006). HA has a depolarizing action within the VN through post-synaptic type 1 or type 2 histamine receptors (H1R or H2R) (Peng et al., 2013), potentially restoring electrophysiological balance, a key parameter in vestibular compensation. HA is known to reduce neuroinflammation in inflammatory contexts (Barata-Antunes et al., 2017; Saraiva et al., 2019), which is particularly relevant given that unilateral vestibular neurectomy (UVN) induces a glial response. In this context, prohistaminergic drugs such as betahistine dihydrochloride (BD) are of interest not only for their potential to alleviate neuroinflammation (Mani and Arfeen, 2024; Yazdi et al., 2020) but also in reducing vestibular syndrome (Lacour, 2013). BD is a partial agonist of H1R and a more potent antagonist of H3 autoreceptors. By blocking H3 autoreceptors, BD increases histamine synthesis in the TMN and release in the VN, thus promoting vestibular compensation in the feline UVN model (see review: Tighilet et al., 2024).

To our knowledge, no study has reported the effect of BD in a UVN rodent model. The very few existing studies have been performed on the rodent model of unilateral labyrinthectomy (Antons et al., 2023; Chen et al., 2019; Fukuda et al., 2021) and confirm the beneficial effect of this pharmacological compound on vestibular compensation. However, the impact of BD on posturo-locomotor components of the vestibular syndrome, as well as on the cellular actors of vestibular function recovery, has not been widely studied.

The present study aims to provide a detailed analysis of the postural and locomotor vestibular syndrome in UVN rats treated with BD while investigating whether BD influences plasticity mechanisms essential for vestibular compensation, including neurogenesis, gliogenesis, inflammation, and neuronal excitability which are known to be modulated by HA (Barata-Antunes et al., 2017; Chen et al., 2019; Saraiva et al., 2019).

2. Material and methods

2.1. Animals

Thirty-one (31) female Long Evans rats of 10–12 weeks old (250/300 g) originating from our own breeding, from parents arising from Charles River (St Germain sur l'Arbresle, France) were used for the experiments. All experiments were performed under veterinary and National Ethical Committee supervision (French Agriculture Ministry Project Authorization: 24,896). The present study was specifically approved by Neurosciences Ethic Committee N°71 of the French National Committee for animal experimentation. Every attempt was made to minimize both the number and the suffering of animals used in the experiment. The animals were housed at the Fédération 3C (Center Saint-Charles, Aix-Marseille University) animal facility, with 12 h–12 h diurnal light variations and free access to water and food. The 31 animals were divided into three groups: SHAM group (n = 7), UVN placebo group (n = 13), UVN BD group (n = 11). See below for the details of procedures and surgery.

2.2. Study design

The 10–12 weeks old female rats were assigned to three groups (SHAM n = 7, UVN placebo n = 13 and UVN BD n = 11) and manipulated for 7 days before unilateral vestibular neurectomy.

For immunohistochemical analysis, a BrdU (bromodeoxyuridine) injection (200 mg/kg, i. p) was performed on rats in the UVN placebo and BD groups 3 days after the neurectomy, which were killed either 2 h

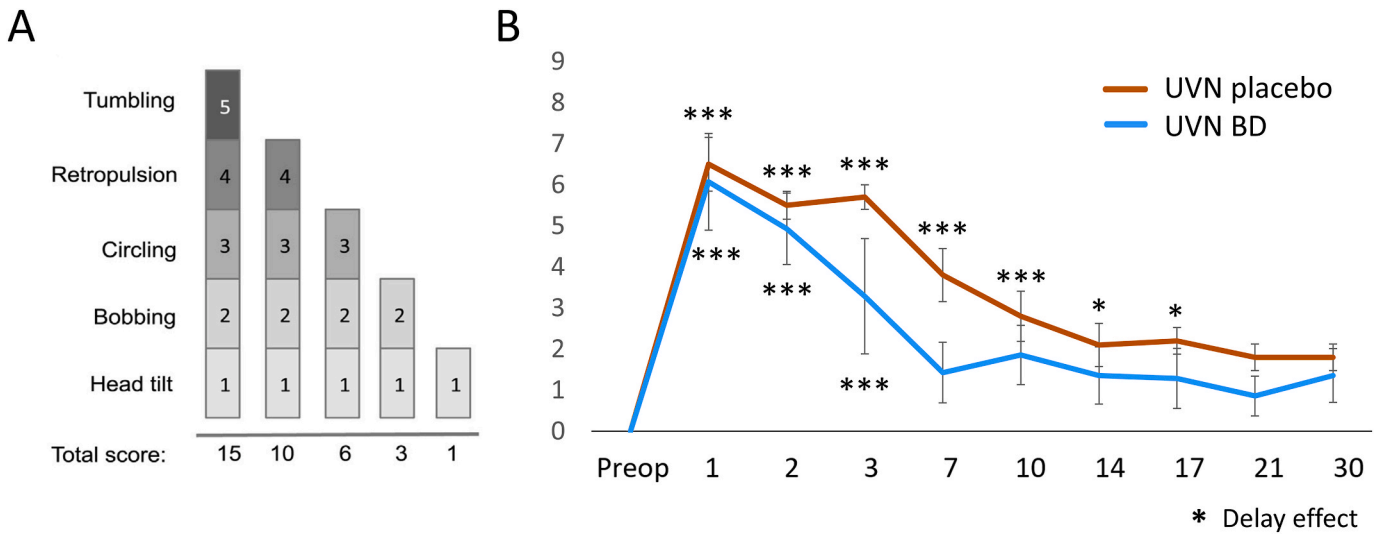

Fig. 2. Qualitative assessment of the posturo-locomotor components of the vestibular syndrome. A. Illustration of the assessment grid used to conduct the analysis (from Péricat et al., 2017). B. Results representing the intensity and kinetics of the vestibular syndrome of the UVN placebo in brown (n = 9) and the UVN BD in blue (n = 7) group from the preoperative session to D30. SHAM group is not represented since these animals do not present any vestibular symptoms. Significant differences are noted * in black for the delay effect. Each point represents the mean for each group ± SEM. Two-way ANOVA with Dunnett's post-hoc test *p < 0.05; **p < 0.01; ***p < 0.001. (For interpretation of the references to colour in this figure legend, the reader is referred to the Web version of this article.)

after the injection (n = 4/group) or 30 days after UVN (n = 4/group). Female rats killed on D3 were not subjected to behavioral tests but were housed under the same conditions as the other groups. In this way, proliferation and short-term effect of treatment (D3 post-UVN) as well as cellular survival and long-term effect of treatment (D30 post-UVN) could be studied.

Behavioral investigations were carried out in two ways (Fig. 1): a quantitative evaluation of the syndrome with the DWB2® (Dynamic Weight Bearing 2) device (Marouane et al., 2020), and a qualitative assessment using the previously published scoring method (Péricat et al., 2017). The behavior of the three groups (SHAM n = 7, UVN placebo n = 9 and UVN BD n = 7) was evaluated on the preoperative session (reference values) and on post-lesion days 1, 2, 3, 7, 10, 14, 17, 21 and 30.

UVN BD groups were treated with 50 mg/kg/day *per os* (p.o) during either three days (n = 4 for immunohistochemical analysis) or ten days for those which underwent behavioral assessment (n = 7). UVN placebo groups underwent the same procedure with 0.9 % sodium chloride solution gavage (in equivalent volume). The dose and duration of treatment were determined based on data from the literature. Several studies show the advantage of high doses of BD administered chronically until the majority of vestibular disorders are compensated (Lacour, 2013; Tighilet et al., 2005). In the UVN cat model, the optimal dose for the synthesis of the enzyme responsible for HA production and improvement of vestibular compensation was 50 mg/kg/day during 3 weeks (Tighilet et al., 1995, 2002, 2005). Since the time course of the vestibular syndrome is divided by two in the UVN rat model (Péricat et al., 2017) and the high plasticity sensitive window takes place in the first post-lesioned week, a ten-day treatment has been administered.

2.3. Surgery

The UVN was performed on UVN placebo (n=13) and UVN BD groups (n=11) following the surgical procedure previously described in the literature (Péricat et al., 2017). Buprenorphine (Buprecare®; 0.05 mg/kg) was given 30 min before the surgery. Rats were deeply anesthetized with isoflurane (4 % concentration for induction and 3 % for maintenance during surgery). Before the animal awakened, a solution of Ringer Lactate (Vibrac; 10 mL/kg) was injected subcutaneously to compensate for possible fluid losses during surgery. The success of the procedure is confirmed upon awakening by the onset of characteristic vestibular symptoms. For the SHAM group (n=7), surgery was stopped at the opening of the tympanic bulla.

2.4. Qualitative assessment of the vestibular syndrome

The vestibular syndrome induced in the rat after UVN is characterized by typical symptoms previously described in various species (rat UVN model: (Marouane et al., 2020; Péricat et al., 2017; Rastoldo et al., 2020), mouse UVN model: (Cassel et al., 2018), cat UVN model (Tighilet et al., 2015)). These symptoms usually include tumbling, retropulsion, circling, bobbing and head-tilt, which are all present in the acute phase of the syndrome and progressively disappear following vestibular compensation.

For this study, we used the same cumulative scale as the one previously reported (Péricat et al., 2017): each symptom has a score based on its severity (tumbling: 5, retropulsion: 4, circling: 3, bobbing: 2, head-tilt: 1) (Fig. 2A).

2.5. Quantitative evaluation of the vestibular syndrome

2.5.1. Analysis device

The second version of the dynamic weight-bearing (DWB2) device (Bioseb, Vitrolles, France) was used to evaluate the postural instability of rodents following unilateral vestibular loss. This apparatus has previously been described for the assessment of postural instabilities in the same model of vestibular loss (Marouane et al., 2020; Tighilet et al., 2017). It consists of a Plexiglas chamber (25 × 25cm) with a floor covered by a 2000 force sensors plate and a high frequency camera above. The weight of each part of the body in contact with the ground was assessed automatically in each sensor at a sampling frequency of 30 Hz. Both the sensors and the camera were connected to a computer using the latest DWB2 software version available at the time (v2.0.60). The same configuration as in our previous studies was used (central pixel weight threshold: 0.7 g, neighbouring pixel weight threshold: 0.3 g, minimum paw size: 2 pixels). Each animal could move freely in the arena for 5 min in each session.

2.5.2. Data analysis

The use of the BIO-ADWB2 features tools and home-made programs

(Scilab) allowed us to extract a wide variety of parameters already described in our previous studies (Marouane et al., 2020, 2021).

The parameters selected for the behavioral assessment of vestibular syndrome are:

- The weight distribution on the left paws (static *vs.* dynamic) which estimates lateral axis imbalance
- The time spent on the abdomen (dynamic), after the identification of each support located between the 4 paws of the animal.
- The average speed of the animal, based on videotracking by the camera.

The following parameters are more specifically related to the static equilibrium of the animals:

- The maximum support surface area, which is the maximum area delimited by the 4 paws of the animal during a session.
- The body sway which is the average of the area of the confidence ellipse at 90 % of the points of the rat's barycenter (which is equivalent to the center of pressure studied in clinical posturology).
- The amount of energy spent for postural stabilization, which is a ratio between the speed of displacement of the barycenter and the body sway.

The barycenter position is calculated for each immobile posture in which the animal stands on all four limbs. Statokinesiograms (Fig. 4A) illustrate the path of the barycenter during an acquisition, as well as the position of the 4 paws of the animal at each moment when the barycenter is calculated. To eliminate inter-individual differences between animals, the posturological results (body sway and amount of energy spent for postural stabilization) and the results relating to average speed were normalized to each animal's results at the pre-operative session.

2.6. Cellular and molecular investigation

2.6.1. Tissue preparation

The rats were anesthetized with a mixture of ketamine (Imalgene 1000®; 100 mg/kg, intraperitoneal) and medetomidine (Domitor®; 0.5 mg/kg, intraperitoneal) and then perfused by intracardiac injection. The intracardiac injection of 400 mL of isotonic saline (0.9 % NaCl) was followed by an injection of 400 mL of a 4 % paraformaldehyde solution (PFA) prepared in 0.1 M phosphate buffer (PB); pH 7.4. At the end of the perfusion, the brain was extracted from the skull and post-fixed for 24 h at 4 °C in the same fixative solution as that used during perfusion. The brains were then rinsed and cryoprotected by successive transfers in increasing concentrations of sucrose (10 %, 20 %, 30 % D-sucrose in 0.1 M PB for 24 h for each bath, 4 °C). Finally, brains were frozen with CO2 gas and cut into 40-μm serial frontal sections with a cryostat (Leica, Wetzlar) for immunohistochemistry. In accordance with the stereotactic atlas of the rat brain (Paxinos and Watson, 2014), 12 serial sections per animal were taken from the beginning of the vestibular nuclei (−9.84 mm from Bregma) to the end of the vestibular nuclei (−13.08 mm from Bregma).

2.6.2. Immunohistochemistry

Immunochemical labeling was performed according to previously validated protocols (Rastoldo et al., 2021; Tighilet et al., 2007a). Floating sections were rinsed in 0.1 M phosphate buffer saline (PBS) (3 × 5min) in multi-well plates. Saturation and permeabilization were achieved by incubation (1 h) in 5 % bovine serum albumin (BSA) and 0.3 % Triton X-100. The sections were then incubated overnight at 4 °C with the following primary antibodies: mouse anti-BrdU (1:100), rabbit anti-NeuN (1:300), rabbit anti-IBA1 (1:2000), goat anti-IBA1 (1:1000), rabbit anti-GFAP (1:200), mouse anti-GFAP (1:200), rabbit anti-Olig2 (1:500), rabbit anti-KCC2 (1:500), and rabbit anti-H1R (1:200). Fluorescent secondary antibodies were used (1:500): Alexa Fluor 594 nm goat anti-mouse, Alexa Fluor 594 nm donkey anti-mouse, Alexa Fluor 594 nm donkey anti-rabbit, Alexa Fluor 488 nm donkey anti-rabbit, and Alexa Fluor 488 nm donkey anti-goat for 2 h at room temperature. During the protocols for the BrdU co-labelings, an incubation with DAPI (1:5000) was performed while it was incorporated into the mounting medium for the other co-labeling. Brain sections were then mounted on SuperFrost®Plus glass slides (Fischer), dried in the dark and at room temperature before mounting with Roti®Mount FluorCare mounting medium with or without DAPI (Carl Roth) according to the protocol.

2.6.3. Cells count

Quantifications of cells expressing specific markers were performed according to previously validated protocols (Dutheil et al., 2013, 2016; Rastoldo et al., 2021; Tighilet et al., 2007a). These observations were made in the deafferented medial vestibular nucleus (MVN) (left side) and in the contralateral MVN (right side) for IBA1 and GFAP immunolabelings. Images were acquired with a Zeiss LM 710 NLO laser scanning confocal microscope equipped with a 63x/1.32NA oil immersion lens that delineates the region of interest by a 425.10 μm^2 square. The average cell counts of the sections obtained after quantification on ImageJ software were used for statistical analysis.

2.6.4. Quantification of KCC2

Image acquisition was performed with a confocal microscope in the left lateral vestibular nucleus (LVN), a vestibular nucleus functionally involved in postural control and containing giant Deiters neurons (100 μm). A program written on Matlab® (Mathworks, Inc) developed to analyze fluorescence at the plasma membrane of neurons was used (Dutheil et al., 2016; El Mahmoudi et al., 2021; Rastoldo et al., 2022). Background or nonspecific immunofluorescence was assessed by calculating the average fluorescence in a selected area devoid of neuron or any other immunolabeled structure. From this region, a threshold equal to the mean immunofluorescence plus three times the standard deviation was defined. All data were then subtracted from this threshold and only positive values were retained for further analysis. A region of interest was then drawn around the plasma membrane of each cell body. The program calculated the average membrane fluorescence in this region of interest on data above 20 % of the maximum value. This threshold was used to ensure that only pixels belonging to the plasma membrane were counted.

2.7. Statistical analysis

For each of the parameters evaluated the recorded values are expressed as mean ± SEM. Concerning the behavioral investigations, we performed Two-way ANOVA with repeated measures to test the effects of BD treatment. Two tests were used for post-hoc analysis. Dunnett's test was performed to compare values at each post-operative time with pre-operative values. Tukey-Kramer multiple comparison test was performed to compare the results obtained between the three groups and between static and dynamic conditions. The Tukey-Kramer multiple comparison test is suited for comparison of samples of different size. To determine the number of animals used for the behavioral assessment in this study, we conducted a power analysis with the G × Power software. We set the effect size at 0.3, since previous work has shown that the effect of BD is easily observable and reproducible. We set the alpha at 0.05 and the power (1-beta) at 0.95 with a group number of 3 and 10 measurements throughout time. The power analysis gives us a total sample size of 21 and therefore, we used 23 rats in total for the behavioral assessment. Concerning the cellular investigations, a one-way ANOVA with a post-hoc Tukey test was performed. P value < 0.05 was considered as statistically significant. *$p < 0.05$, **$p < 0.01$, ***$p < 0.001$.

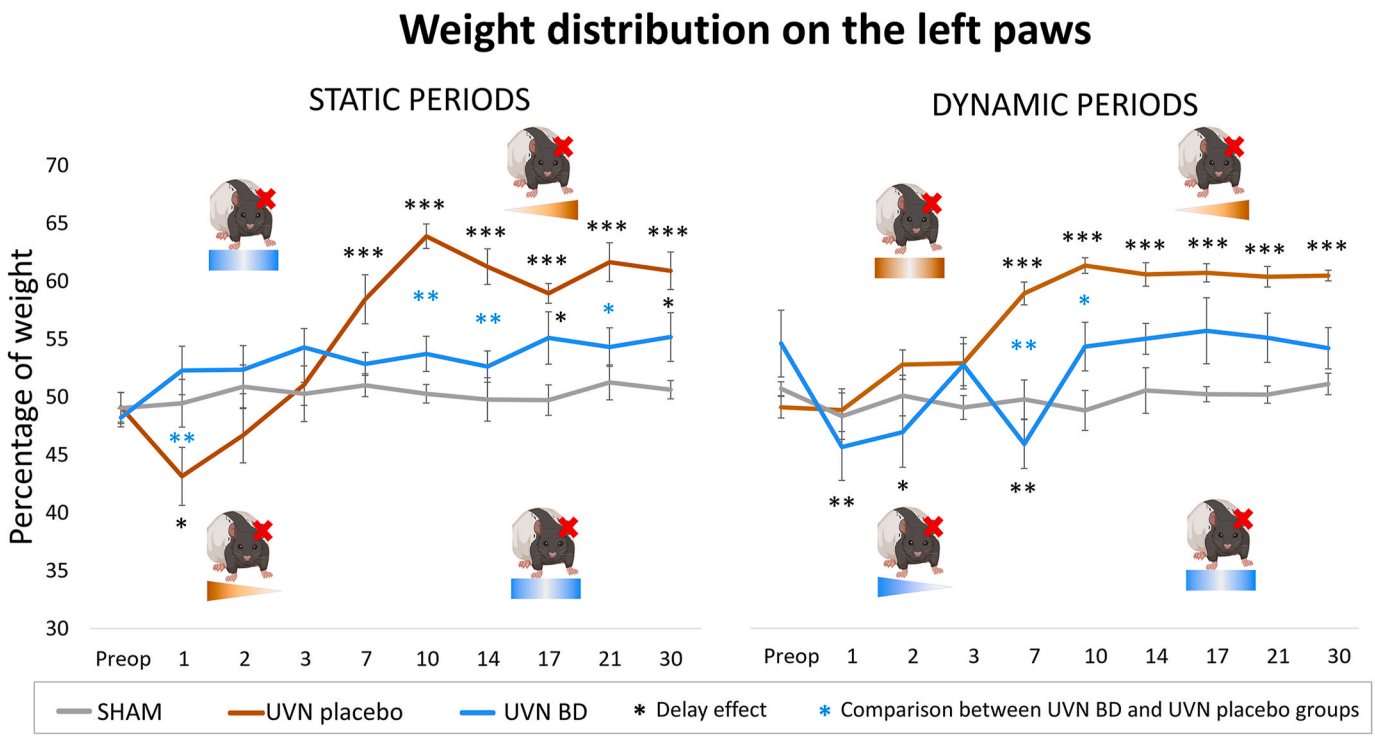

Fig. 3. Weight distribution along the lateral axis. This parameter highlights the muscle tone deficits of the three groups of animals. The SHAM group (n = 7) shows a perfectly balanced weight distribution between the right and the left, without any influence of the surgery in static and dynamic periods. In the UVN placebo group (n = 9), there is a shift of the static weight to the right at D1 ($p < 0.05$) but the dynamic weight distribution is well balanced in the acute phase of the vestibular syndrome. At compensated delays, the UVN placebo group applied significantly more weight to the left in both static and dynamic conditions (delay effect: $p < 0.001$). From the preoperative session to D14, the weight distribution of the UVN BD group (n = 7) shows a pattern close to that of the SHAM group in static condition. From D17 onwards, this group shifts its weight to the left (delay effect at D17 and D30, $p < 0.05$), but in a less pronounced way than the UVN placebo group (statistical difference between the two groups at D21, $p < 0.05$). In the dynamic condition, the UVN BD group shifts its weight to the right in the critical period (delay effect at D1, D2 and D7, $p < 0.05$) but recovers its dynamic lateral balance from D10. Each point represents the mean for each group ± SEM. Two-way ANOVA with Dunnett's post-hoc test × $p < 0.05$; **$p < 0.01$; ***$p < 0.001$.

3. Results

3.1. Behavioral results

3.1.1. Qualitative assessment of the effect of betahistine treatment

Qualitative assessment of the vestibular syndrome showed no difference between groups (Two-way ANOVA, time x group factor: $F(9, 126) = 1.288$; $p = 0.249$) but a difference in the kinetics of syndrome expression (Two-way ANOVA, time factor: $F(9, 126) = 35.82$; $p < 0.0001$). At D1, both the UVN placebo group and the UVN BD group showed a peak in the expression of the vestibular syndrome (UVN placebo: 6.5 ± 0.65; BD: 6.07 ± 1.18) (Fig. 2B). For the UVN placebo group, the vestibular disorders progressively decreased from day 7 to day 30 but the delay effect persisted in this group until day 17 (from D1 to D10: $p < 0.001$, from D14 to D17: $p < 0.05$). In the group treated with BD, the delay effect was only present in the critical period (from D1 to D3: $p < 0.001$) and most of the disorders disappeared as early as D7 (disappearance of the delay effect). However, no significant differences appeared between the two groups.

3.1.2. Quantitative evaluation of betahistine effect on the posturolocomotor component of the vestibular syndrome

3.1.2.1. Lateral weight distribution. Fig. 3 shows a different time course of weight distribution between the 3 groups studied (Two-way ANOVA: $F(45, 360) = 4.509$; $p < 0.0001$). In the SHAM group, under static and dynamic conditions, the animal distributes its weight equally on the left side (about 50 % throughout the session). In the static condition, the UVN placebo group shows a different behavioral phenotype. During the critical period, it applies more weight to the right in static condition (delay effect at D1, $p < 0.05$). During the compensated period of the syndrome, the UVN placebo group significantly balances its weight on the left in static condition ($p < 0.001$ from D10 to D30). The weight distribution observed in the UVN BD group was close to the SHAM group in static condition. No statistical difference was observed between these two groups and the weight applied on the left side varied little despite a slight increase at the end of the compensation period (delay effect, $p < 0.05$ at D17 and D30). Furthermore, statistical analysis revealed a significant difference between the two groups UVN placebo and UVN BD in the acute period of the syndrome (D1: $p < 0.01$) but also in the compensated period of the syndrome (D10 and D14: $p < 0.01$; D21: $p < 0.05$). In the dynamic condition, the UVN placebo group balanced correctly during the critical period while it balanced its weight on the left during the compensated period. The UVN BD group applied more weight to the right at D1 ($p < 0.01$) and D2 ($p < 0.05$) post-UVN than in the preoperative delay, but without showing significant differences with the other two groups. Unlike the UVN placebo group, the UVN BD group favored a right-sided weight distribution at D7 (delay effect: $p < 0.01$). A significant difference was observed between these two groups at D7 ($p < 0.01$) and persisted until D10 ($p < 0.05$). The UVN BD group then distributed between 50 and 55 % of its weight to the left on average from D14 to D30. At these delays, no difference was noted between the three groups in dynamic condition.

3.1.2.2. Static behavior. The static balance of the animals was assessed using posturological parameters. In Fig. 4A, we can observe the stato-kinesiograms of animals belonging to the SHAM, UVN placebo and UVN BD groups at D1 and D30 post-surgery. On the first post-injury day the

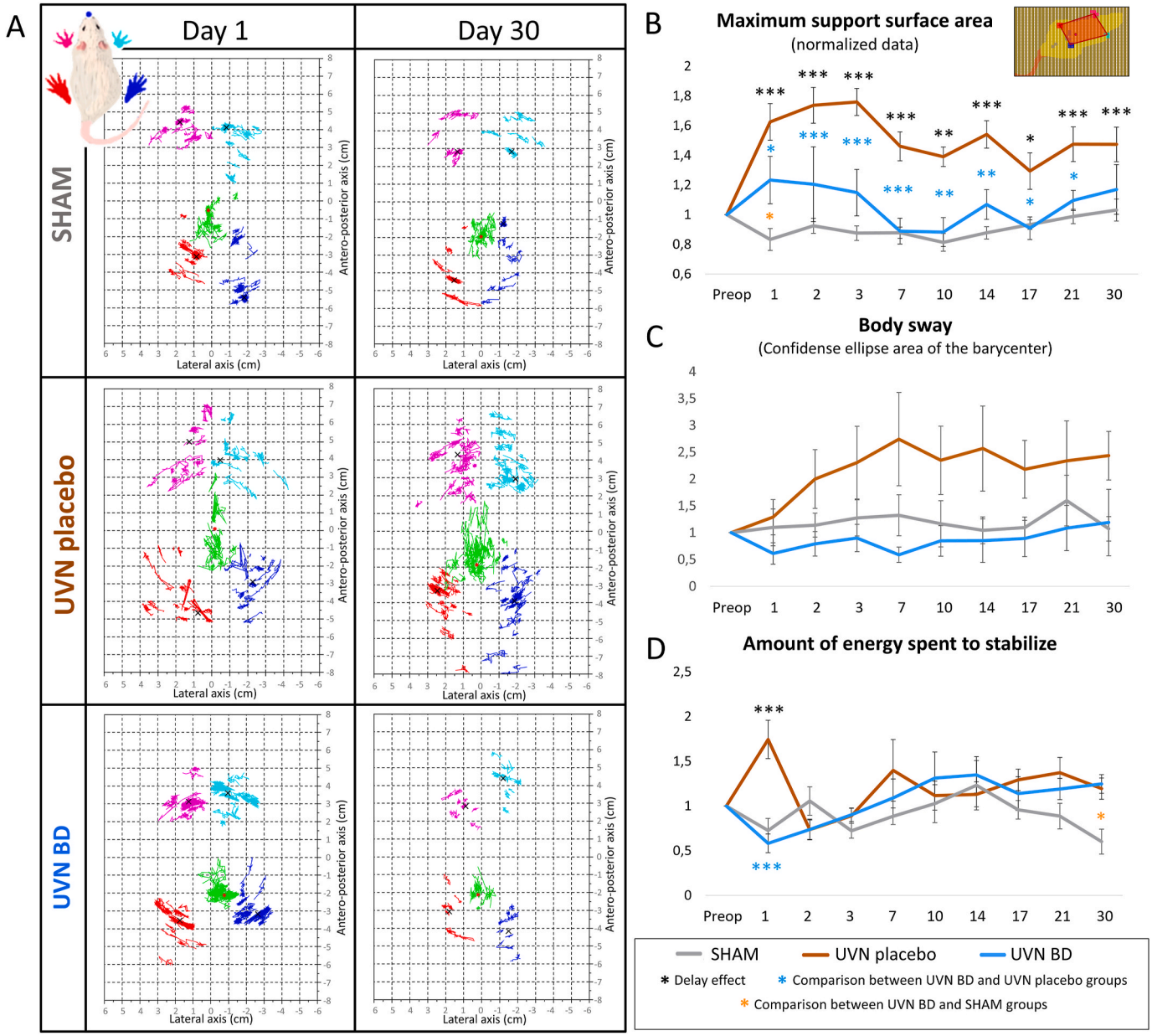

Fig. 4. Posturographic parameters. A. Rodent statokinesiograms: representation of the kinetics of the successive positions of the animals' paws and the barycenter. The different lines indicate the group of the animal from which the plot is extracted, and the columns indicate the acquisition time (day 1 and day 30 post-op). At day 1, the plot of the UVN BD group (n = 7) shows less instability than the UVN placebo group (n = 9) and seems like that of the SHAM group (n = 7). At D30, the statokinesiograms of the SHAM and UVN BD groups seemed identical, whereas the instability seemed to persist in the UVN placebo group. The following parameters quantify postural instability in the rodent. B. Maximum support surface area. This parameter increased significantly at D1 in the UVN placebo group, and never returned to baseline. It remained stable in the SHAM group. The UVN BD group slightly increased its maximum support surface area at D1 but quickly returned to control values. C. The body sway highlights an instability that progressively sets in for the UVN placebo group and that lasts. The SHAM and UVN BD groups managed to maintain their postural stability at all postoperative time points. D. Amount of energy spent to stabilize. From the preoperative session to post-injury day 21, the evolution of this parameter is similar for the UVN BD group and the SHAM group until D17. At D1, the UVN placebo group spent significantly more energy than the other groups ($p < 0.001$) and showed a delay effect ($p < 0.001$). At D30, the UVN BD and the UVN placebo group expend significantly more energy to stabilize than the SHAM groups. Each point represents the mean for each group ± SEM. Two-way ANOVA with Dunnett's post-hoc test × $p < 0.05$; **$p < 0.01$; ***$p < 0.001$.

vestibular disorders were at their peak and at D30 the animals have compensated the majority of these disorders in this rodent model of unilateral vestibulopathy (Marouane et al., 2020; Péricat et al., 2017; Rastoldo et al., 2020; Tighilet et al., 2017). Plots from the SHAM group appear relatively similar between D1 and D30. In the UVN placebo group, the clouds were more dispersed at these two times. An instability seemed to set in and last until 30 days post-UVN. The statokinesiograms of the UVN BD group looked more like those of the SHAM group with less dispersed point clouds, and a relatively small sustentation polygon.

The following parameters allowed the quantification of rodent postural balance from statokinesiogram data.

3.1.2.2.1. Maximum support surface area. The UVN BD group adopted a different behavioral phenotype than the two other groups (Two-way ANOVA: $F(18, 180) = 3.197$; $p < 0,0001$). The maximum support surface area decreased slightly at D1 and then remained stable in the SHAM group during all sessions (Fig. 4B). In the UVN placebo group, the maximum support surface area increased significantly from D1 (delay effect: $p < 0.001$) and remained significantly high until the

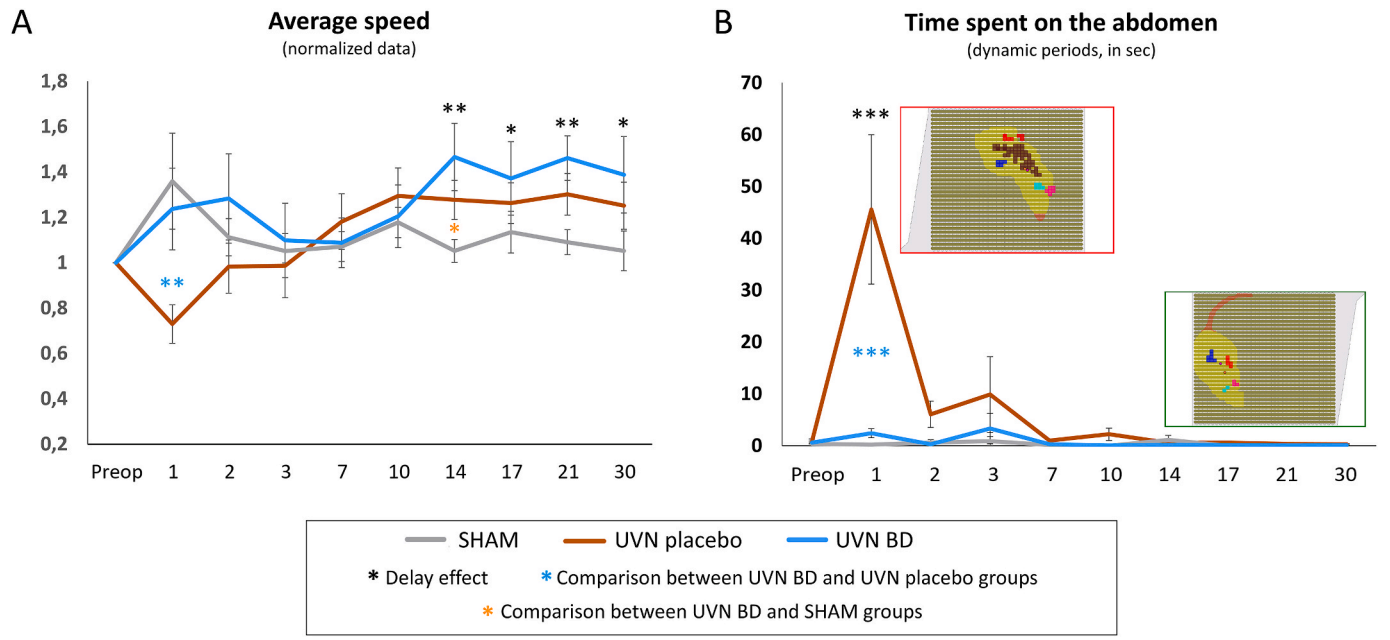

Fig. 5. Dynamic behavior. This figure summarizes the dynamic behavior of the animals when they are in the DWB2. A. Average speed. In the SHAM (n = 7) and UVN BD groups (n = 7), the average speed of the animals increased in the critical period, while it decreased in the UVN placebo group (n = 9) (significant difference between the UVN BD and UVN groups at D1, $p < 0.01$). In the compensated period, animals in the UVN BD group seem to exhibit hyperactivity characterized by a delay effect from D14 to D30 ($p < 0,05$) and a significant increase compaired to the UVN placebo group at D14 ($p < 0.05$). B. Time spent on the abdomen. The UVN placebo group showed an increased spend more time on the abdomen during the critical period (delay effect, and significant differences with the UVN BD group at D1, $p < 0.001$). This behavior was not observed in the other two groups. Each point represents the mean for each group ± SEM. Two-way ANOVA with Dunnett's post-hoc test × $p < 0.05$; **$p < 0.01$; ***$p < 0.001$.

end of the compensated period (D2 to D7, D14, D21 and D30: $p < 0.001$; D10: $p < 0.01$; D17: $p < 0.05$). In the UVN BD group, the maximum support surface area increased slightly at D1 and showed a significant difference with the SHAM group for which a slight decrease occurred at the same time ($p < 0.05$). This parameter then decreased at D2 and returned to control values for the compensated periods. No delay effect was observed for the UVN BD group and the maximum support surface area of the UVN BD group was significantly lower from D1 to D21 compared with the UVN placebo group (D1, D17 and D21: $p < 0.05$; D2 to D7: $p < 0.001$; D10 to D14: $p < 0.01$).

3.1.2.2.2. Body sway. For the SHAM group and the UVN BD group, the body sway varied very little and is around 1 throughout the post-operative stages (Fig. 4C). In contrast, the body sway seemed to increase progressively from D1 to D3 in the UVN placebo group. This parameter reflects what was observed in the statokinesiograms but, probably due to the high variability, the results of statistical tests do not show significant differences (Two-way ANOVA: $F(18, 180) = 1.375$; $p = 0.1486$).

3.1.2.2.3. Amount of energy spent to stabilize. A ratio between the speed of displacement of the barycentre and its dispersion surface allowed us to have an estimate of the amount of energy spent to stabilize with the appearance of significant differences in statistical tests (Fig. 4D, Two-way ANOVA: $F(18, 180) = 2.931$; $p < 0.0001$). A peak of energy was observed at D1 in the UVN placebo group (delay effect: $p < 0.001$), where a significant difference appeared in comparison with the UVN BD group. In the three groups of the study, the kinetics of change in this parameter were equivalent from D2 to D21. Between D21 and D30, the amount of energy expended to stabilize decreased slightly for the SHAM group, without any delay effect. In the UVN placebo group and the UVN BD group, the values obtained at D21 and D30 were very close to the preoperative values. At D30, a difference appeared between the SHAM group and the UVN BD group ($p < 0.05$), due to the decrease observed in the SHAM group.

3.1.2.3. Dynamic behavior

3.1.2.3.1. Average speed. The average speed of the SHAM, UVN placebo and UVN BD groups showed different kinematics (Fig. 5A, Two-way ANOVA: $F(18, 180) = 2.757$; $p = 0.0003$). As early as D1 post-UVN, a decrease in mean velocity was observed in the UVN placebo group, concomitant with an increase in the average speed of the SHAM and UVN BD groups. The results of the UVN placebo and UVN BD groups were significantly different at this time point ($p < 0.01$). From D2 to D10, the average speed of the three groups was then relatively similar. It was close to the preoperative values and no statistical difference was observed during this period. The results of the SHAM group varied little until D30 and remained close to 1 (normalized data). From D14 to D30, the UVN placebo group's velocity was on average higher than that of the SHAM group, without showing any statistical difference. During this period, the velocity of the UVN BD group was higher than that of the UVN placebo group. Compared to the SHAM group, the average speed of the UVN BD group was significantly higher at D14 ($p < 0.05$). A delay effect also appeared and persisted from D14 to D30 (D14 and D21: $p < 0.01$, D17 and D30: $p < 0.05$).

3.1.2.3.2. Time spent on the abdomen. At D1, animals in the UVN placebo group applied significantly more time on their abdomen in dynamic periods than before surgery ($p < 0.001$) and in comparison, with the other two groups ($p < 0.001$) (Fig. 5B, Two-way ANOVA: $F(18, 180) = 5.551$, $p < 0.0001$). From D2 post-UVN, this time decreased drastically, and these significant differences disappeared. From D7 to D30 the animals of the UVN groups no longer put their abdomen on the sensors in dynamic condition. The SHAM group, as well as the UVN BD group, did not put their abdomen on the sensors during the dynamic periods, or did so in a negligible way.

3.2. Cellular results

3.2.1. Betahistine dihydrochloride reduces microglial and astrocytic response in the deafferented medial vestibular nucleus

The results obtained from the behavioral analyses show that BD treatment accelerates vestibular compensation and suggest an effect of

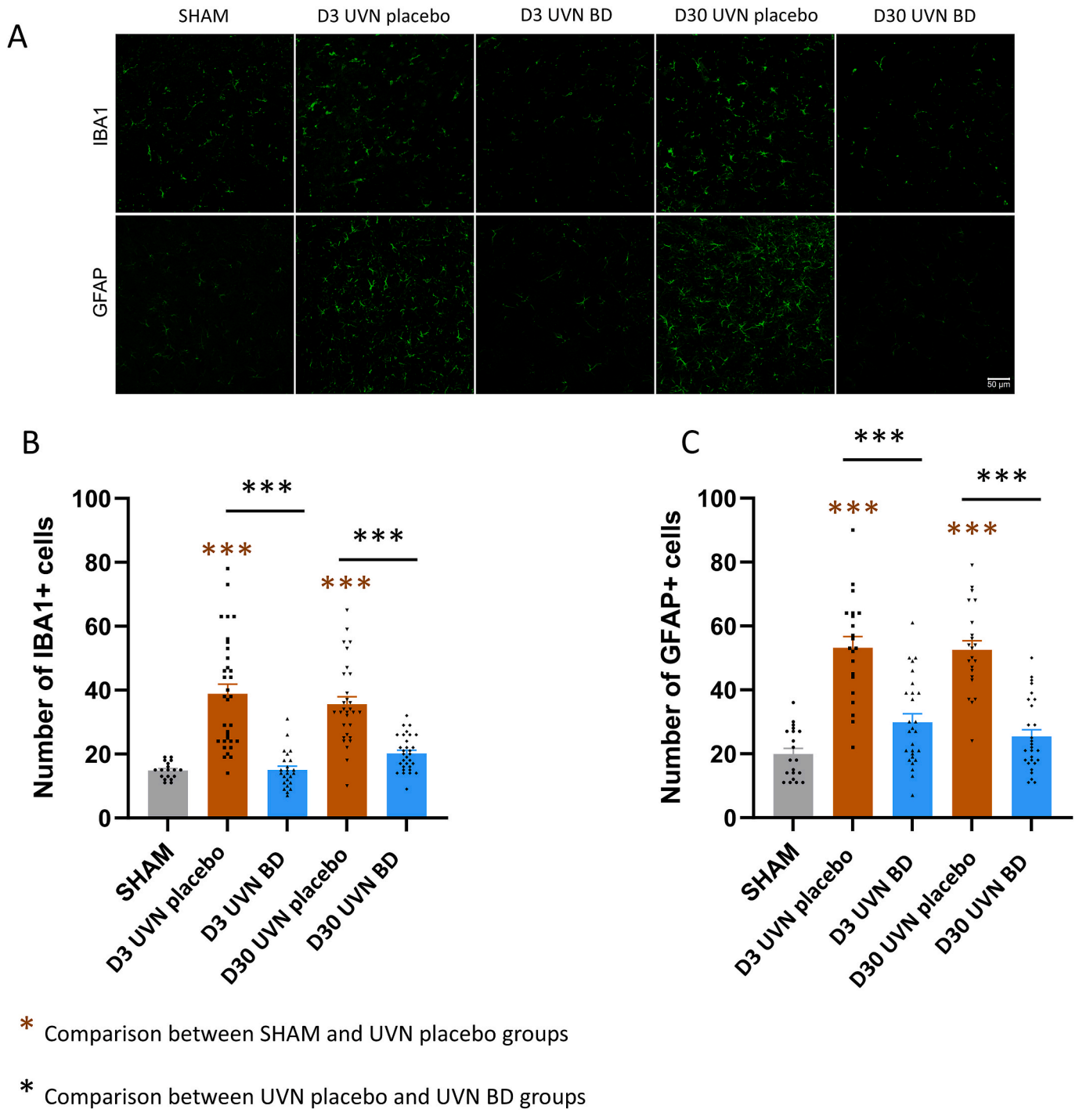

Fig. 6. Betahistine dihydrochloride treatment attenuates astrocytic (GFAP) and microglial (IBA1) immunostaining in the deafferented medial vestibular nucleus (MVN) after UVN. A. Confocal immunostaining images of IBA1+ and GFAP + cells in the left MVN of SHAM group, three days (D3) or thirty days (D30) after UVN for UVN placebo and UVN BD groups (n = 4/groups). Scale bar 50 µm. B and C. Quantitative evaluations of the effect of betahistine dihydrochloride treatment and UVN on the number of IBA1+ (B) and GFAP+ (C) cells in the deafferented MVN of the UVN placebo (brown) and UVN BD (blue) groups sacrificed three days or thirty days after the lesion compared to the SHAM group (grey). A significant difference is indicated by * in brown for the difference between the SHAM group and the UVN placebo group and by * in black for the difference between the UVN placebo group and the UVN BD group. The histograms represent the mean for each group ± SEM and each point corresponds to the number of cells in each image analyzed. One-way ANOVA with Tukey post-hoc test ***$p < 0.001$. (For interpretation of the references to colour in this figure legend, the reader is referred to the Web version of this article.)

this pro-histaminergic compound at the level of central structures processing vestibular information. In a first step, we sought to confirm the presence of the H1R, one of the targets of this treatment, in VN. We demonstrated the presence of this receptor on the different cell types involved in vestibular compensation, such as microglia (IBA1+/H1R+), astrocytes (GFAP/H1R+) (Supplementary Data 1). Immunohistochemical investigations regarding the number of microglial cells (IBA1 antibody) and the number of astrocytic cells (GFAP antibody) revealed a significant decrease in the deafferented MVN of the UVN BD group (Fig. 6A) but no significant difference in the opposite MVN (Supplementary Data 2). Statistical analyses highlight a significant increase in microglia (Fig. 6B, One-way ANOVA: $F(4, 131) = 29.59$; $p <$

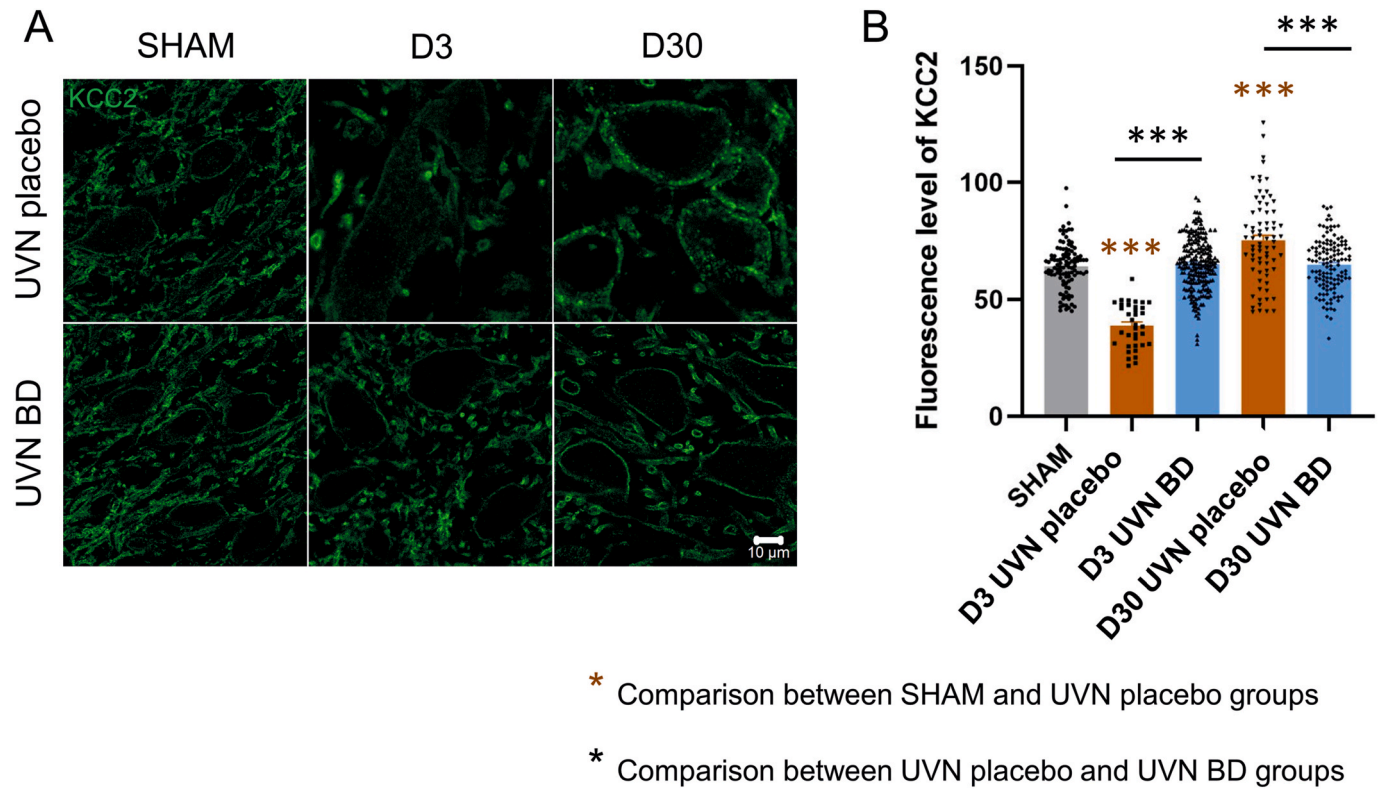

Fig. 7. Betahistine dihydrochloride treatment normalizespotassium-chloride co-transporter KCC2 expression in the deafferented lateral vestibular nucleus after UVN. A. Confocal immunostaining images in the left lateral vestibular nucleus (LVN) showing the KCC2 staining (green) in vestibular neurons of SHAM group, three days (D3) or thirty days (D30) after UVN for UVN placebo and UVN BD groups (n = 4/groups). Scale bar 10 µm. B. Quantification of membrane labeling density in vestibular neurons of SHAM rats (grey), UVN placebo (brown) and UVN BD (blue) groups at either D3 or D30 after UVN. A significant difference is indicated by * in brown for the difference between the SHAM group and the UVN placebo group and by * in black for the difference between the UVN placebo group and the UVN BD group. The histograms represent the mean for each group ± SEM and each point corresponds to the number of cells in each image analyzed. One-way ANOVA with Tukey post-hoc test ***$p < 0.001$.***$p < 0.001$. (For interpretation of the references to colour in this figure legend, the reader is referred to the Web version of this article.)

0.0001) and astrocytes (Fig. 6C, One-way ANOVA: $F(4, 113) = 32.83$; $p < 0.0001$) in UVN placebo group at D3 (GFAP: $p < 0.001$; IBA1: $p < 0.001$) and D30 (GFAP: $p < 0.001$; IBA1: $p < 0.001$) compared to the SHAM group. This increase was not found in the UVN BD group (no significant difference with the SHAM group). Moreover, a significant decrease in the number of microglial and astrocytic cells was found for the UVN BD group compared to the UVN placebo group at D3 (GFAP and IBA1: $p < 0.001$) and D30 (GFAP: $p < 0.001$; IBA1: $p < 0.001$).

3.2.2. Betahistine dihydrochloride prevents downregulation of the potassium-chloride co-transporter KCC2 in the deafferented lateral vestibular nucleus

Immunostaining for the potassium-chloride co-transporter KCC2 in the LVN from the SHAM, UVN placebo, and UVN BD groups is shown in Fig. 7A. Statistical difference has been shown between groups (One-way ANOVA for $F(4, 544) = 56.04$; $p < 0.0001$). Although we confirmed decreased KCC2 immunoreactivity in the deafferented LVN of the UVN placebo group at D3 post-lesion survival time compared with the control group ($p < 0.001$). No difference was found for the UVN BD group compared with the SHAM group regardless of the survival time considered (Fig. 7B). Furthermore, we found a significant increase in KCC2 expression level for UVN BD group compared to UVN placebo group at D3 post-lesion survival time ($p < 0.001$), which was reversed at D30 post-lesion survival time ($p < 0.001$).

3.2.3. Betahistine dihydrochloride remodulates cell proliferation and gliogenesis

BrdU immunostaining in MVN from the SHAM, UVN placebo, and UVN BD groups is shown Fig. 8A. Statistical difference has been shown between groups (One-way ANOVA for $F(4, 100) = 10.55$; $p < 0.0001$). A significant increase in the number of BrdU+ cells was observed at D3 post-lesion survival time in the deafferented MVN of the UVN placebo group ($p < 0.01$) and the UVN BD group ($p < 0.001$) (Fig. 8B). At D30 post-lesion survival time, both the UVN placebo group and the UVN BD group showed a significant increase in BrdU labeling ($p < 0.001$). Finally, a significant increase in cell proliferation was observed in the UVN BD compared to the UVN placebo group (D3, $p < 0.05$) but not for cell survival (D30) between the UVN placebo and UVN BD group.

BrdU/GFAP, IBA1, Olig2, and NeuN immunostaining in deafferented MVN is shown in Fig. 8D. In the deafferented MVN from the UVN placebo group, our results showed a homogeneous proportion of the different cell types (around 25 %) (Fig. 8E). In the deafferented MVN of the UVN BD group, we observed an increase in the number of BrdU+/IBA1+ cells (39 % *vs.* 24 %) at the expense of the number of BrdU+/NeuN + cells (13 % *vs.* 28 %) (Fig. 8F).

4. Discussion

This study highlights for the first time the effect of BD in a rodent model of acute unilateral vestibulopathy at both the behavioral and cellular level. BD is a partial agonist of histamine H1 receptors and a more potent antagonist of histamine H3 autoreceptors. We show an acceleration of vestibular compensation with a significant improvement of postural-locomotor parameters in vestibular lesioned animals treated with BD. This behavioral effect is thought to be underpinned by BD's cellular effects in the vestibular nuclei, including a microgliogenesis as

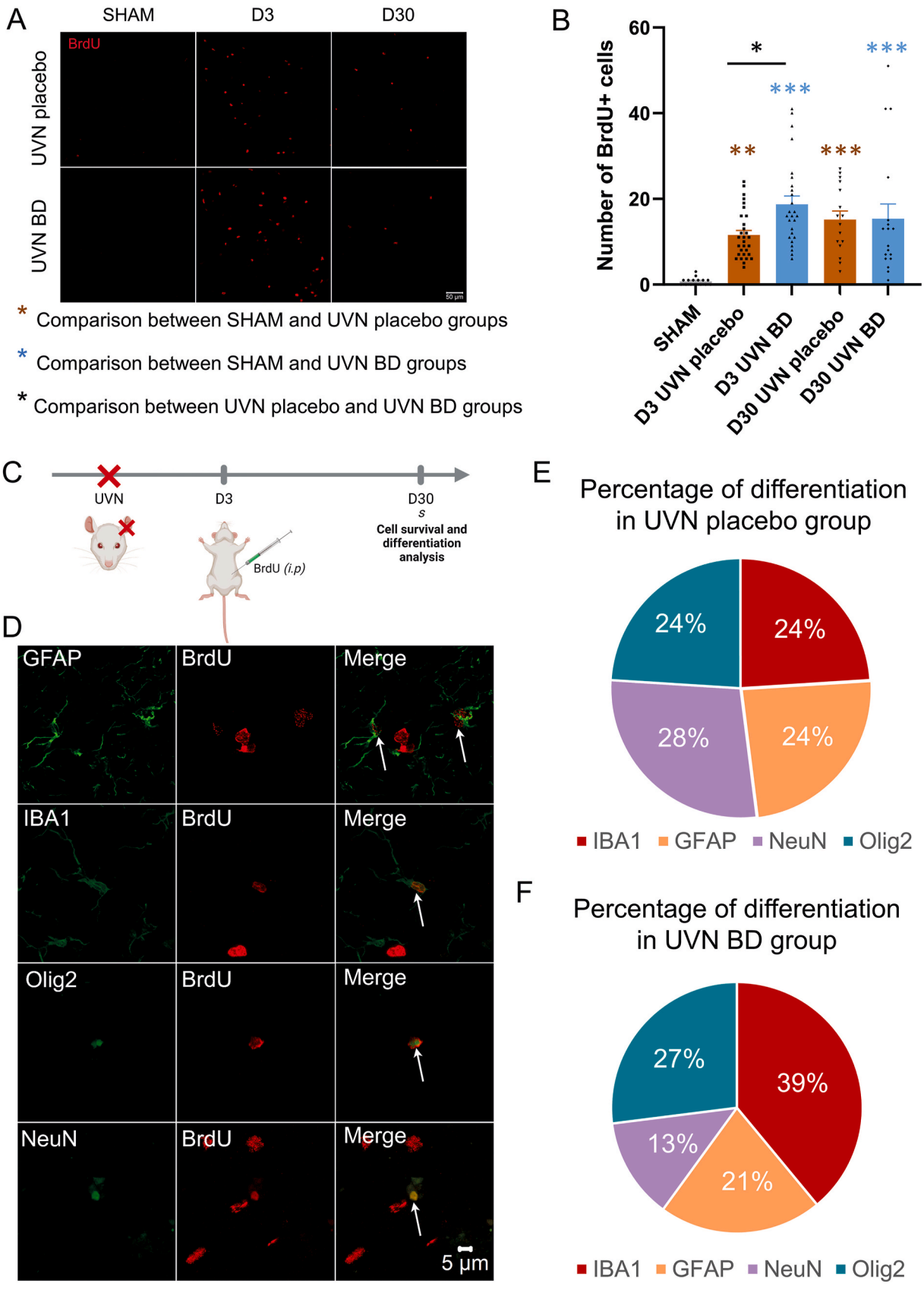

(caption on next page)

Fig. 8. Betahistine dihydrochloride and cell proliferation survival and differentiation in the deafferented medial vestibular nucleus after UVN. A. Confocal immunostaining images of BrdU+ cells in the left MVN of SHAM group, three days (D3) or thirty days (D30) after UVN for placebo and UVN BD groups (n = 4/groups). Scale bar 50 μm. B. Quantitative evaluations of the effect of betahistine treatment and UVN on the number of BrdU+ cells in the deafferented MVN of the UVN placebo (brown) and UVN BD (blue) groups sacrificed three days or thirty days after the lesion compared to the SHAM group (grey). A significant difference is indicated by * in brown for the difference between the SHAM group and the UVN placebo group and by * in blue for the difference between the SHAM group and the UVN BD group and * in black for the difference between the UVN placebo group and the UVN BD group. The histograms represent the mean for each group ± SEM and each point corresponds to the number of cells in each image analyzed. One-way ANOVA with Tukey post-hoc test × $p < 0.05$, **$p < 0.01$, ***$p < 0.001$. C. Illustration of the protocol used to study the fate of newly generated cells in MVN thirty day after UVN. BrdU is injected three days after UVN and the quantification of survival cell is carried out thirty days after UVN. UVN: unilateral vestibular neurectomy, i. p: intraperitoneal injection, s: sacrifice. D. Maximum intensity projection of z-stack confocal images of cell differentiation evaluated in the deafferented MVN thirty days after UVN. The BrdU nuclei are in red, and the other markers of differentiation are: GFAP (astrocyte), IBA1 (microglia), oligodendrocyte (Olig2), neuron (NeuN) are in green. Scale bar = 10 μm. E and F. Pie charts illustrating the percentage of GFAP, IBA1, NeuN and Olig2+ cells among the BrdU+ cells in the UVN placebo (E) and UVN BD (F) groups. (For interpretation of the references to colour in this figure legend, the reader is referred to the Web version of this article.)

well as a modulation of excitability and cells responsible for inflammation (microglial cells and astrocytes).

4.1. Use of an automated behavioral device to validate the effectiveness of a betahistine dihydrochloride treatment

4.1.1. Betahistine dihydrochloride induces rapid compensation of static deficits

The static deficits appear when the subjects are immobile and are likely a behavioral consequence of the electrophysiological imbalance between the VN (Lacour et al., 2016). In patients with unilateral vestibular deafferentation, BD improves and accelerates recovery of static symptoms (Redon et al., 2011). Our data underline a recovery of the static deficits in the UVN BD group during the critical period, consistent with the results obtained in the feline UVN model (Tighilet et al., 1995, 2007b, 2018) and in unilabyrinthectomized rats (Chen et al., 2019).

Weight shifting towards the ipsilesional side was assimilated to a compensatory strategy already observed in this rodent model of vestibulopathy (Facchini et al., 2021; Marouane et al., 2020; Tighilet et al., 2017). BD-treated animals did not exhibit any shift towards the ipsilesional side as observed with another pharmacological compound which accelerates vestibular compensation (Rastoldo et al., 2022).

The maximum support surface area, a crucial parameter for postural stabilization, reveals that BD-treated animals maintain their base of support, demonstrating enhanced stability. Furthermore, the amount of energy spent to stabilize required by the BD-treated group is similar to that of the sham group, in contrast to the UVN placebo group, which shows a substantial increase on the first day following injury. The treatment would have allowed a more rapid rebalancing of the electrophysiological balance between the vestibular nuclei, thus limiting the behavioral deficits persisting in the long term after the lesion.

4.1.2. Static compensation during the critical period is followed by improved dynamic recovery

The dynamic data reflect the complexity of the dynamic vestibular compensation mechanisms which rely mainly on sensory substitution mechanisms (Lacour et al., 2016).

Despite little evidence in the rodent model, a faster improvement of dynamic balance following BD treatment was demonstrated with the rotarod test (Chen et al., 2019) as already shown in the UVN feline model with the rotating beam device (Tighilet et al., 1995, 2007b). In contrast to these motor tests, our evaluation of the dynamic behavior is ecological and based on the natural behavior of rodents. The rehabilitative effects of the rotarod or rotating beam could improve the compensation of dynamic vestibular disorders through reorganization in cerebral motor networks (Scholz et al., 2015). Consistent with this, studies in humans have shown that rehabilitation protocol improves long-term dynamic balance through modulation of cerebral networks (Karapolat et al., 2010).

The average speed increased in the UVN BD group as early as the first day post-injury to 30 days after the lesion. This hyperactivity induced by BD treatment was also observed by Antons et al. in a dose-dependent manner (Antons et al., 2023). This increased activity may be mediated by an agonist action of BD on H1R or by histamine. Indeed, reduced locomotor activity has been found in H1R KO mice (Schneider et al., 2014) and in vestibulo-lesioned animals treated with mepyramine, an H1R antagonist (Chen et al., 2019).

During the critical period, we observed a contralesional lateral weight shift in BD-treated animals. This weight imbalance could be induced by the circling behavior of the animals: while rotating to the left, the animals are mainly supported on their right legs. However, contrary to the UVN placebo group, treated animals do not put their abdomen on the ground, indicating a better dynamic balance induced by the BD treatment. In the compensated period, the weight distribution of BD-treated animals is balanced in a similar way to the SHAM group, unlike the UVN placebo group, which distribute more weight towards the ipsilesional side. Thus, despite some locomotor deficits observed in the critical period, BD-treated animals show an improved dynamic balance compared to the UVN group.

Our results demonstrate a rapid action of BD on static postural deficits that might result from electrophysiological rebalancing between both vestibular nuclei complexes (VNCs). In addition, BD's prohistamniergic action on motor brain structures may increase locomotor activity, promoting compensation for dynamic deficits.

4.2. Modulation of betahistine dihydrochloride on cellular vestibular post-lesion plasticity

4.2.1. Betahistine dihydrochloride decreases the number of glial cells responsible for neuroinflammation in the deafferented medial vestibular nucleus

IBA1+ and GFAP + cells, which are considered as markers for active microglia and reactive astrocytes (Karve et al., 2016), are significantly upregulated in the deafferented MVN after UVN. These observations are in agreement with previous studies indicating the proinflammatory effect of UVN in both rodent (El Mahmoudi et al., 2021) and feline (Dutheil et al., 2016) models. Given the crucial role of glial cells in neuroinflammation, understanding their response to UVN is essential for identifying potential therapeutics.

The dual role of HA in inflammation and on glial cells is well documented, with HA exhibiting pro- and anti-inflammatory effects in physiological and inflammatory environments, respectively (Barata-Antunes et al., 2017; Ferreira et al., 2012; Saraiva et al., 2019). Since both microglia and astrocytes express histamine receptors (HR) (Dong et al., 2014; Xu et al., 2018) and microglia are known to produce HA (Katoh et al., 2001), these cells are frontline to exhibit pro- and anti-inflammatory effects.

BD treatment significantly reduces the number of GFAP+ and IBA1+ cells in the MVN following UVN, indicating a reduction of neuroinflammation as already demonstrated in another model (Shalaby et al., 2022). Our result is in line with the anti-inflammatory effect of HA in an inflammatory environment. Thus, BD modulates glial activation and potentially exerts an anti-inflammatory effect in this model (Shalaby

et al., 2022). This effect could be mediated through the signaling cascade triggered by H3R blockade induced by BD (Arrang et al., 1985). Since both microglia and astrocytes express H3R (Barata-Antunes et al., 2017), its blockade by BD could activate the cAMP/PKA/CREB signaling cascade which is known to reduce glial-mediated inflammation (Wang et al., 2022).

In addition to its anti-inflammatory action, BD would facilitate vestibular compensation by also using other mechanisms such as rebalancing VN activity which is considered as a crucial parameter of vestibular function recovery.

4.2.2. *Betahistine dihydrochloride promotes vestibular nuclei excitability*

4.2.2.1. Betahistine dihydrochloride promotes vestibular nuclei excitability via neuronal H1 and H2 receptors. After deafferentation, the priority of the deafferented vestibular environment is to restore a level of homeostatic excitability essential for functional recovery. In this mission, agents that modulate neuronal excitability play a key role.

We demonstrated that the deafferented vestibular environment recapitulates a developmental stage such that GABA becomes depolarizing through a transient reduction of KCC2 co-transporters and that this effect might facilitate vestibular function recovery (Dutheil et al., 2016; Rastoldo et al., 2022). In the present study, the expression of KCC2 co-transporters is unchanged in UVN rats treated with BD. This pharmacological compound thus prevents the internalization of KCC2 co-transporters considered as an energy-consuming process. In response to deafferentation, the deafferented VN shift from a depolarizing GABAergic strategy (KCC2 internalization) to an excitatory mechanism driven by endogenous HA (Li et al., 2017; Wang and Dutia, 1995; Zhang et al., 2008), whose release is strongly promoted by BD treatment (Tighilet et al., 2002). Indeed, by blocking H3R autoreceptor and activating H1R in the deafferented VN, BD increases HA endogenous synthesis in the TMN and release in the VN. This massive HA release in the deafferented VN promotes the readjustment of the electrophysiological balance between the VNCs by depolarizing action of HA on H1R and H2R located on the excitatory vestibular neurons (Chen et al., 2019; Li et al., 2017; Wang and Dutia, 1995; Zhang et al., 2008). In addition, BD by itself has a depolarizing action in H1R. In support of this argument a recent study revealed an increase in cerebral glucose metabolism in the deafferented VN of unilabyrinthectomized (UL) rats subjected to high doses of BD (Antons et al., 2023). This increase in energy metabolism occurring during the acute phase would reflect an increase in spontaneous activity in ipsilateral VN inducing electrophysiological rebalancing between the VNCs and thus restoration of balancing function. Chen et al. also emphasize the depolarizing action of both HA and BD on GABAergic commissural interneurons to restore the electrophysiological balance between the VNCs and thus accelerate vestibular compensation (Chen et al., 2019).

4.2.2.2. Betahistine dihydrochloride promotes vestibular nuclei plasticity. Given that vestibular compensation can be seen as sensorimotor relearning (Facchini et al., 2021), synaptic plasticity must be required. This effect could be achieved via H1R activation, either activated through BD agonist action or by the increase in HA conferred by BD. H1R activation might lead to increased DAG and IP3 which activate PKC and elevate intracellular calcium, respectively known to be key factors in the induction of the early stages of synaptic plasticity in the hippocampus (Haas and Panula, 2003).

Following vestibular deafferentation, VN are deprived of peripheral excitability. Thus, restoring excitability in the deafferented VN through intrinsic reorganization is necessary for vestibular compensation. According to a recent study by Akiyoshi et al. microglia, by contact on dendritic spines, increases synaptic activity and synchronization of neuronal populations. This effect is absent in an inflammatory context (Akiyoshi et al., 2018). Thus, BD, acting as an anti-inflammatory compound in our inflammatory lesion context, could allow the restoration of the synchronizing effect of the neural networks. Furthermore, the release of anti-inflammatory cytokines IL-4 can induce microglia to produce BDNF (Zhang et al., 2021), a key factor in plasticity and vestibular compensation (Dutheil et al., 2016).

4.2.3. *Betahistine dihydrochloride modulates cell proliferation and gliogenesis*

Our results demonstrated that BD increases cell proliferation during acute vestibular syndrome, without impacting the level of cell survival at post-injury D30. Consistent with our findings, a recent study in mice showed that LPS-induced inflammation in the hippocampus, followed by HA injection, significantly increased cell proliferation (Saraiva et al., 2019). Without treatment, after one month, survival cells in the MVN differentiate into neurons or glial cells in equal proportions, consistent with previous findings of our team (Marouane et al., 2021; Rastoldo et al., 2022). We show, for the first time, that BD treatment favors microglial differentiation among newly generated cells at 3 days post-lesion. Elevated neuronal HA levels induced by BD may promote microglial differentiation with neuroprotective properties in the deafferented VN. This neuroprotective role could be attributed to microglial-derived BDNF, which has already shown its neuroprotective effect in cerebral ischemia (Lee et al., 2002).

Prominent microgliogenesis is consistently observed one month post-surgery, whether compensation is enhanced by pharmacological intervention or sensorimotor rehabilitation (Marouane et al., 2021; Rastoldo et al., 2022). Our study confirms this pattern once more, suggesting that microglia play a crucial role in vestibular compensation, serving as a primary target for various therapeutic strategies.

4.3. *Translation of betahistine dihydrochloride on cellular vestibular post-lesion plasticity*

BD is widely used for the treatment of various vestibular disorders in clinical practice, including its administration following acute unilateral vestibular loss to foster vestibular compensation. Similar to the settings of this experimental study, selective vestibular neurectomy is applied in humans as an ultimate treatment for vestibular schwannoma or intractable Menière's disease. A recent randomized controlled trial in 124 patients showed a dose-dependent improvement of balance and a higher proportion of full resolution of spontaneous nystagmus on day 14 after vestibular neurectomy by intranasal BD as compared to placebo (Van de Heyning et al., 2023). Another prospective clinical trial found an acceleration of improvement across various clinical endpoints (including body sway, spontaneous nystagmus, subjective visual vertical) by 24 mg BD b. i.d. compared to placebo after unilateral vestibular neurectomy in patients (Redon et al., 2011). These high-quality clinical data indicate an accelerated and enhanced vestibular compensation, which nicely resembles the observation of the current experimental model.

In clinical settings, the most common cause of acute peripheral vestibular loss is a vestibular neuritis, which likely originates from the reactivation of latent herpes viruses in the primary vestibular afferents (Himmelein et al., 2017; Rujescu et al., 2020). Compared to vestibular neurectomy, the deafferentation in vestibular neuritis is incomplete in most cases. Glial activation was seen along the vestibular nerve and in the vestibular nucleus on the lesion side in patients 3–10 days after vestibular neuritis by in vivo molecular imaging with the tspo-ligand [18 F]GE180 (unpublished data). This finding is comparable to similar glial activations in an animal model of unilateral labyrinthectomy (Zwergal et al., 2017). Given the action of BD on glial activation reported in the current study, it seems conceivable that this drug – besides its other actions on neurotransmission and neuronal activity - can modulate neuroinflammatory processes towards an augmentation of vestibular compensation mechanisms also in the context of vestibular neuritis in humans. Importantly, a successful translation of experimental findings from animal models to clinical application requires a specific

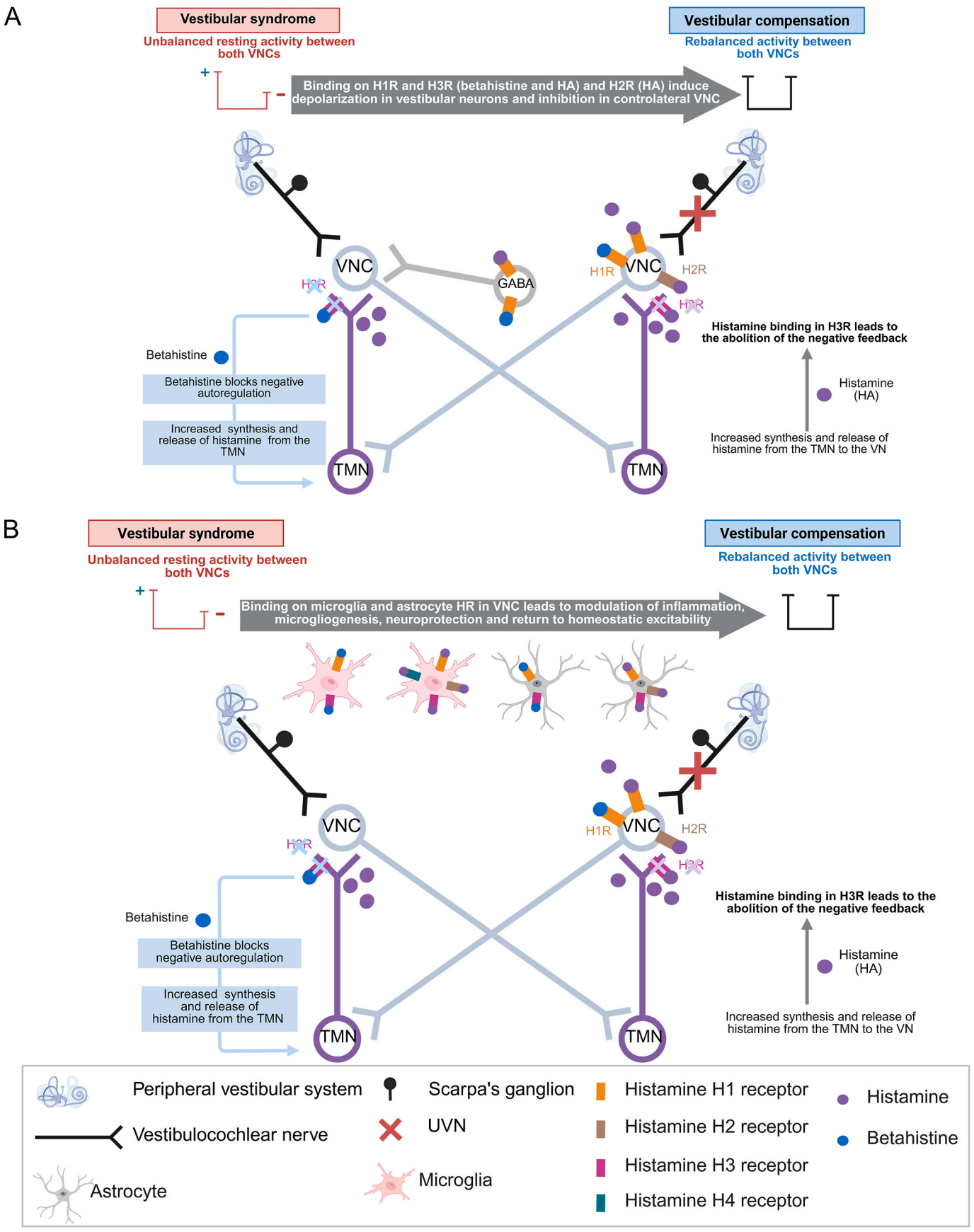

(caption on next page)

Fig. 9. Explanatory model describing the influence of betahistine on the balance between the two vestibular nuclei complexes (VNCs) after unilateral vestibular nerve deafferentation regarding neurons (A) or glial cells (B). A: betahistine dihydrochloride and histamine actions on neuronal histaminergic receptors located in the vestibular nuclei complex after unilateral vestibular neurectomy (UVN). The tuberomamillary nuclei (TMN) located in the posterior hypothalamus send ipsilateral histaminergic projections to each VNC. The VNCs also receive excitatory afferents from peripheral vestibular receptors. Post-synaptic type 1 (H1R) and type 2 histamine receptors (H2R) are present in the vestibular nuclei under basal conditions and excite neurons present in the VNCs. Presynaptic type 3 histamine receptors (H3R) present on afferents from TMNs mediate autoregulation of brain histamine synthesis and release in the VNC. These different mechanisms of excitation and autoinhibition allow maintenance of the balance between the two VNCs. UVN leads to a decrease in the excitability of the ipsilateral VNC, resulting in an unbalanced resting activity between the two VNCs. This electrophysiological imbalance prompts increased histamine synthesis and release in the deafferented VNC. Betahistine dihydrochloride (BD) increases these effects by blocking negative autoregulation by H3R. Histamine (HA) and BD binding to H1R and H3R, as well as HA binding to H2R, induce depolarization in vestibular neurons. This activity also triggers inhibition in contralateral vestibular nuclei complex via GABAergic commissural interneurons, leading to a balanced resting activity between the two VNCs. B: betahistine dihydrochloride and histamine actions on glial histaminergic receptors located in the vestibular nuclei complex after unilateral vestibular neurectomy. UVN leads to a decrease in the excitability of the ipsilateral VNC, resulting in an unbalanced resting activity between the two VNCs. This electrophysiological imbalance prompts increased histamine synthesis and release in the deafferented VNC. BD increases these effects by blocking negative autoregulation by H3R. Binding to H1R, H2R, H3R, H4R on microglia receptors and to H1R, H2R, H3R on astrocyte receptors in the deafferented VNC leads to the modulation of inflammation, microgliogenesis, neuroprotection and maintenance of homeostatic excitability. These different plasticity mechanisms will allow, among other things, to restore the balance between the two VNCs during vestibular compensation.

consideration of differences in BD bioavailability as a result of its application route. While BD in animal models is often administered parenterally, in clinical practice this drug is currently available only as an oral preparation. BD p. o. is metabolized by enteric and hepatic MAO-B enzymes by 99 %. Thus, active BD blood level in this case is below those of experimental models using i. v. application. In consequence, some controlled clinical trials with oral application of BD have failed to show therapeutic benefits against placebo (Adrion et al., 2016). Future clinical trials therefore aim to apply BD intranasaly (Van de Heyning et al., 2023) or combine oral BD with a MAO-B inhibitor such as selegiline or rasagiline, which results in up to 100-fold higher plasma concentrations (Strupp et al., 2023). Application protocols optimized towards higher BD plasma levels may be the key to a successful translation of the promising experimental findings to therapeutic benefits in clinical application.

4.4. Implications and limitations

While in clinical use for decades, the pharmacological action of BD has not been fully deciphered yet. The current study adds an important mechanism of action for this drug, which goes beyond the previous hypothesis of a change of histaminergic neurotransmission. It also highlights the importance of a decrease of microglia related inflammation in the process of successful central vestibular compensation. As most types of acute unilateral vestibulopathy in human medicine are considered to be caused by an inflammation of the vestibular nerve with secondary microglial activation in the vestibular nucleus, the here reported therapeutic effects of BD do nicely align with this pathophysiology. On the other hand, some limitations remain: while not testing BD in animals without vestibular impairment could be considered a limitation, existing evidence suggests that BD has minimal influence on the intact VN (Wang and Dutia, 1995). Additionally, the absence of significant glial reactivity in the contralesional vestibular nuclei (see Supplementary Data 2) supports our decision to exclude BD treatment in sham rats. Furthermore, a causal relationship of the BD effects on microglia activity during vestibular compensation needs to be established in future experiments. In this respect the co-application of BD with minocycline or Pexidartinib to inhibit microglia activation or to deplete microglia would be of interest. Another limitation for the translation of results to patients may be that we are currently lacking direct evidence for cell proliferation in the vestibular nuclei area in humans.

5. Conclusion

Our study demonstrates that BD accelerates vestibular compensation by significantly improving posturo-locomotor parameters in vestibular lesioned animals. BD treatment might facilitate vestibular compensation through histamine-mediated modulation of inflammation and neuroprotection in the VN, promoting electrophysiological rebalancing (Fig. 9).

CRediT authorship contribution statement

Jessica Trico: Writing – review & editing, Writing – original draft, Methodology, Investigation, Formal analysis, Data curation, Conceptualization. **Emna Marouane:** Writing – review & editing, Writing – original draft, Methodology, Investigation, Formal analysis, Data curation, Conceptualization. **Isabelle Watabe:** Methodology, Investigation. **Agnes Lapotre:** Methodology. **Alain Tonetto:** Methodology. **Andreas Zwergal:** Writing – review & editing, Writing – original draft, Visualization, Validation, Supervision. **Christian Chabbert:** Visualization, Validation, Resources. **Brahim Tighilet:** Writing – review & editing, Writing – original draft, Visualization, Validation, Supervision, Methodology, Investigation, Funding acquisition, Conceptualization.

Funding

This research was supported by grants from the Ministère de l'Enseignement Supérieur et de la Recherche and CNRS (UMR 7260 and UMR 7077 Aix-Marseille Université).

Declaration of competing interest

The authors declare the following financial interests/personal relationships which may be considered as potential competing interests: Brahim Tighilet reports financial support was provided by Aix-Marseille University. If there are other authors, they declare that they have no known competing financial interests or personal relationships that could have appeared to influence the work reported in this paper.

Acknowledgments

We thank Elodie Mansour for taking care of the animals and Abdessadek El Ahmadi for expertise in statistical analysis. We would like to thank Théo Armand-Hilaire for his help in analyzing the histological data and Guillaume Rastoldo for proofreading.

Appendix A. Supplementary data

Supplementary data to this article can be found online at https://doi.org/10.1016/j.ejphar.2025.177600.

Data availability

Data will be made available on request.

References

Adrion, C., Fischer, C.S., Wagner, J., Gürkov, R., Mansmann, U., Strupp, M., BEMED Study Group, 2016. Efficacy and safety of betahistine treatment in patients with Meniere's disease: primary results of a long term, multicentre, double blind, randomised, placebo controlled, dose defining trial (BEMED trial). BMJ 352, h6816. https://doi.org/10.1136/bmj.h6816.

Akiyoshi, R., Wake, H., Kato, D., Horiuchi, H., Ono, R., Ikegami, A., Haruwaka, K., Omori, T., Tachibana, Y., Moorhouse, A.J., Nabekura, J., 2018. Microglia enhance synapse activity to promote local network synchronization. eNeuro 5. https://doi.org/10.1523/ENEURO.0088-18.2018. ENEURO.0088-18.2018.

Antons, M., Lindner, M., Eilles, E., Günther, L., Delker, A., Branner, C., Krämer, A., Beck, R., Oos, R., Wuehr, M., Ziegler, S., Strupp, M., Zwergal, A., 2023. Dose- and application route-dependent effects of betahistine on behavioral recovery and neuroplasticity after acute unilateral labyrinthectomy in rats. Front. Neurol. 14, 1175481. https://doi.org/10.3389/fneur.2023.1175481.

Arrang, J.M., Garbarg, M., Quach, T.T., Tuong, M.D.T., Yeramian, E., Schwartz, J.-C., 1985. Actions of betahistine at histamine receptors in the brain. Eur. J. Pharmacol. 111, 73–84. https://doi.org/10.1016/0014-2999(85)90115-3.

Barata-Antunes, S., Cristóvão, A.C., Pires, J., Rocha, S.M., Bernardino, L., 2017. Dual role of histamine on microglia-induced neurodegeneration. Biochim. Biophys. Acta (BBA) - Mol. Basis Dis. 1863, 764–769. https://doi.org/10.1016/j.bbadis.2016.12.016.

Cassel, R., Bordiga, P., Pericat, D., Hautefort, C., Tighilet, B., Chabbert, C., 2018. New mouse model for inducing and evaluating unilateral vestibular deafferentation syndrome. J. Neurosci. Methods 293, 128–135. https://doi.org/10.1016/j.jneumeth.2017.09.002.

Chen, Z.-P., Zhang, X.-Y., Peng, S.-Y., Yang, Z.-Q., Wang, Y.-B., Zhang, Y.-X., Chen, X., Wang, J.-J., Zhu, J.-N., 2019. Histamine H1 receptor contributes to vestibular compensation. J. Neurosci. 39, 420–433. https://doi.org/10.1523/JNEUROSCI.1350-18.2018.

Dong, H., Zhang, W., Zeng, X., Hu, G., Zhang, H., He, S., Zhang, S., 2014. Histamine induces upregulated expression of histamine receptors and increases release of inflammatory mediators from microglia. Mol. Neurobiol. 49, 1487–1500. https://doi.org/10.1007/s12035-014-8697-6.

Dutheil, S., Brezun, J.M., Leonard, J., Lacour, M., Tighilet, B., 2009. Neurogenesis and astrogenesis contribution to recovery of vestibular functions in the adult cat following unilateral vestibular neurectomy: cellular and behavioral evidence. Neuroscience 164, 1444–1456. https://doi.org/10.1016/j.neuroscience.2009.09.048.

Dutheil, S., Escoffier, G., Gharbi, A., Watabe, I., Tighilet, B., 2013. GABA $_A$ receptor agonist and antagonist alter vestibular compensation and different steps of reactive neurogenesis in deafferented vestibular nuclei of adult cats. J. Neurosci. 33, 15555–15566. https://doi.org/10.1523/JNEUROSCI.5691-12.2013.

Dutheil, S., Watabe, I., Sadlaoud, K., Tonetto, A., Tighilet, B., 2016. BDNF signaling promotes vestibular compensation by increasing neurogenesis and remodeling the expression of potassium-chloride cotransporter KCC2 and GABA $_A$ receptor in the vestibular nuclei. J. Neurosci. 36, 6199–6212. https://doi.org/10.1523/JNEUROSCI.0945-16.2016.

El Mahmoudi, N., Rastoldo, G., Marouane, E., Péricat, D., Watabe, I., Tonetto, A., Hautefort, C., Chabbert, C., Sargolini, F., Tighilet, B., 2021. Breaking a dogma: acute anti-inflammatory treatment alters both post-lesional functional recovery and endogenous adaptive plasticity mechanisms in a rodent model of acute peripheral vestibulopathy. J. Neuroinflammation 18, 183. https://doi.org/10.1186/s12974-021-02222-y.

Facchini, J., Rastoldo, G., Xerri, C., Péricat, D., El Ahmadi, A., Tighilet, B., Zennou-Azogui, Y., 2021. Unilateral vestibular neurectomy induces a remodeling of somatosensory cortical maps. Progress in Neurobiology 205, 102119. https://doi.org/10.1016/j.pneurobio.2021.102119.

Ferreira, R., Santos, T., Gonçalves, J., Baltazar, G., Ferreira, L., Agasse, F., Bernardino, L., 2012. Histamine modulates microglia function. J. Neuroinflammation 9, 90. https://doi.org/10.1186/1742-2094-9-90.

Fukuda, J., Matsuda, K., Sato, G., Kitahara, T., Matsuoka, M., Azuma, T., Kitamura, Y., Tomita, K., Takeda, N., 2021. Effects of betahistine on the development of vestibular compensation after unilateral labyrinthectomy in rats. Brain Sci. 11, 360. https://doi.org/10.3390/brainsci11030360.

Haas, H., Panula, P., 2003. The role of histamine and the tuberomamillary nucleus in the nervous system. Nat. Rev. Neurosci. 4, 121–130. https://doi.org/10.1038/nrn1034.

Himmelein, S., Lindemann, A., Sinicina, I., Horn, A.K.E., Brandt, T., Strupp, M., Hüfner, K., 2017. Differential involvement during latent Herpes simplex virus 1 infection of the superior and inferior divisions of the vestibular ganglia: implications for vestibular neuritis. J. Virol. 91, e00331. https://doi.org/10.1128/JVI.00331-17, 17.

Karapolat, H., Celebisoy, N., Kirazli, Y., Bilgen, C., Eyigor, S., Gode, S., Akyuz, A., Kirazli, T., 2010. Does betahistine treatment have additional benefits to vestibular rehabilitation? Eur. Arch. Otorhinolaryngol. 267, 1207–1212. https://doi.org/10.1007/s00405-010-1216-0.

Karve, I.P., Taylor, J.M., Crack, P.J., 2016. The contribution of astrocytes and microglia to traumatic brain injury. Br. J. Pharmacol. 173, 692–702. https://doi.org/10.1111/bph.13125.

Katoh, Y., Niimi, M., Yamamoto, Y., Kawamura, T., Morimoto-Ishizuka, T., Sawada, M., Takemori, H., Yamatodani, A., 2001. Histamine production by cultured microglial cells of the mouse. Neurosci. Lett. 305, 181–184. https://doi.org/10.1016/S0304-3940(01)01835-3.

Lacour, M., 2013. Betahistine treatment in managing vertigo and improving vestibular compensation: clarification. J. Vestib. Res. 23, 139–151. https://doi.org/10.3233/VES-130496.

Lacour, M., Helmchen, C., Vidal, P.-P., 2016. Vestibular compensation: the neuro-otologist's best friend. J. Neurol. 263, 54–64. https://doi.org/10.1007/s00415-015-7903-4.

Lacour, M., Tighilet, B., 2010. Plastic events in the vestibular nuclei during vestibular compensation: the brain orchestration of a "deafferentation" code. Restor. Neurol. Neurosci. 28, 19–35. https://doi.org/10.3233/RNN-2010-0509.

Lee, T.-H., Kato, H., Chen, S.-T., Kogure, K., Itoyama, Y., 2002. Expression disparity of brain-derived neurotrophic factor immunoreactivity and mRNA in ischemic hippocampal neurons. Neuroreport 13, 2271–2275. https://doi.org/10.1097/00001756-200212030-00020.

Li, B., Zhang, X.-Y., Yang, A.-H., Peng, X.-C., Chen, Z.-P., Zhou, J.-Y., Chan, Y.-S., Wang, J.-J., Zhu, J.-N., 2017. Histamine increases neuronal excitability and sensitivity of the lateral vestibular nucleus and promotes motor behaviors via HCN channel coupled to H2 receptor. Front. Cell. Neurosci. 10, 300. https://doi.org/10.3389/fncel.2016.00300.

Mani, V., Arfeen, M., 2024. Betahistine's neuroprotective actions against lipopolysaccharide-induced neurotoxicity: insights from experimental and computational studies. Brain Sci. 14, 876. https://doi.org/10.3390/brainsci14090876.

Marouane, E., El Mahmoudi, N., Rastoldo, G., Péricat, D., Watabe, I., Lapôtre, A., Tonetto, A., Xavier, F., Dumas, O., Chabbert, C., Artzner, V., Tighilet, B., 2021. Sensorimotor rehabilitation promotes vestibular compensation in a rodent model of acute peripheral vestibulopathy by promoting microgliogenesis in the deafferented vestibular nuclei. Cells 10, 3377. https://doi.org/10.3390/cells10123377.

Marouane, E., Rastoldo, G., El Mahmoudi, N., Péricat, D., Chabbert, C., Artzner, V., Tighilet, B., 2020. Identification of new biomarkers of posturo-locomotor instability in a rodent model of vestibular pathology. Front. Neurol. 11.

Matsuyama, T., Kayahara, T., Nomura, J., Nakano, K., 1996. Direct projections from the medial vestibular nucleus to the posterior hypothalamic area in the monkey (Macaca fuscata). Neurosci. Lett. 219, 199–202. https://doi.org/10.1016/s0304-3940(96)13206-7.

Paxinos, G., Watson, C., 2014. Paxino's and Watson's the Rat Brain in Stereotaxic Coordinates, seventh ed. Elsevier/AP, Academic Press is an imprint of Elsevier, Amsterdam ; Boston.

Peng, S.-Y., Zhuang, Q.-X., He, Y.-C., Zhu, J.-N., Wang, J.-J., 2013. Histamine excites neurons of the inferior vestibular nucleus in rats by activation of H1 and H2 receptors. Neurosci. Lett. 541, 87–92. https://doi.org/10.1016/j.neulet.2013.02.040.

Péricat, D., Farina, A., Agavnian-Couquiaud, E., Chabbert, C., Tighilet, B., 2017. Complete and irreversible unilateral vestibular loss: a novel rat model of vestibular pathology. J. Neurosci. Methods 283, 83–91. https://doi.org/10.1016/j.jneumeth.2017.04.001.

Rastoldo, G., El Mahmoudi, N., Marouane, E., Pericat, D., Watabe, I., Toneto, A., López-Juárez, A., Chabbert, C., Tighilet, B., 2021. Adult and endemic neurogenesis in the vestibular nuclei after unilateral vestibular neurectomy. Progress in Neurobiology 196, 101899. https://doi.org/10.1016/j.pneurobio.2020.101899.

Rastoldo, G., Marouane, E., El Mahmoudi, N., Péricat, D., Bourdet, A., Timon-David, E., Dumas, O., Chabbert, C., Tighilet, B., 2020. Quantitative evaluation of a new posturo-locomotor phenotype in a rodent model of acute unilateral vestibulopathy. Front. Neurol. 11.

Rastoldo, G., Marouane, E., El-Mahmoudi, N., Péricat, D., Watabe, I., Lapotre, A., Tonetto, A., López-Juárez, A., El-Ahmadi, A., Caron, P., Fraysse, M.-J.E., Chabbert, C., Zwergal, A., Tighilet, B., 2022. L-Thyroxine improves vestibular compensation in a rat model of acute peripheral vestibulopathy: cellular and behavioral aspects. Cells 11, 684. https://doi.org/10.3390/cells11040684.

Redon, C., Lopez, C., Bernard-Demanze, L., Dumitrescu, M., Magnan, J., Lacour, M., Borel, L., 2011. Betahistine treatment improves the recovery of static symptoms in patients with unilateral vestibular loss. J. Clin. Pharmacol. 51, 538–548. https://doi.org/10.1177/0091270010369241.

Rujescu, D., Herrling, M., Hartmann, A.M., Maul, S., Giegling, I., Konte, B., Strupp, M., 2020. High-risk allele for Herpes labialis severity at the IFNL3/4 locus is associated with vestibular neuritis. Front. Neurol. 11. https://doi.org/10.3389/fneur.2020.570638.

Saraiva, C., Barata-Antunes, S., Santos, T., Ferreiro, E., Cristóvão, A.C., Serra-Almeida, C., Ferreira, R., Bernardino, L., 2019. Histamine modulates hippocampal inflammation and neurogenesis in adult mice. Sci. Rep. 9, 8384. https://doi.org/10.1038/s41598-019-44816-w.

Schneider, E.H., Neumann, D., Seifert, R., 2014. Modulation of behavior by the histaminergic system: lessons from H1R-and H2R-deficient mice. Neurosci. Biobehav. Rev. 42, 252–266. https://doi.org/10.1016/j.neubiorev.2014.03.009.

Scholz, J., Niibori, Y., W Frankland, P., P Lerch, J., 2015. Rotarod training in mice is associated with changes in brain structure observable with multimodal MRI. Neuroimage 107, 182–189. https://doi.org/10.1016/j.neuroimage.2014.12.003.

Shalaby, A.M., Sharaf Eldin, H.E.M., Abdelsameea, A.A., Abdelnour, H.M., Alabiad, M.A., Elkholy, M.R., Aboregela, A.M., 2022. Betahistine attenuates seizures, neurodegeneration, apoptosis, and gliosis in the cerebral cortex and hippocampus in a mouse model of epilepsy: a histological, immunohistochemical, and biochemical study. Microsc. Microanal. 1–15. https://doi.org/10.1017/S1431927622012107.

Smith, P.F., Curthoys, I.S., 1988a. Neuronal activity in the contralateral medial vestibular nucleus of the Guinea pig following unilateral labyrinthectomy. Brain Res. 444, 295–307. https://doi.org/10.1016/0006-8993(88)90938-9.

Smith, P.F., Curthoys, I.S., 1988b. Neuronal activity in the ipsilateral medial vestibular nucleus of the Guinea pig following unilateral labyrinthectomy. Brain Res. 444, 308–319. https://doi.org/10.1016/0006-8993(88)90939-0.

Strupp, M., Churchill, G.C., Naumann, I., Mansmann, U., Al Tawil, A., Golentsova, A., Goldschagg, N., 2023. Examination of betahistine bioavailability in combination

with the monoamine oxidase B inhibitor, selegiline, in humans-a non-randomized, single-sequence, two-period titration, open label single-center phase 1 study (PK-BeST). Front. Neurol. 14, 1271640. https://doi.org/10.3389/fneur.2023.1271640.

Tighilet, B., Brezun, J.M., Dit Duflo Sylvie, G., Gaubert, C., Lacour, M., 2007a. New neurons in the vestibular nuclei complex after unilateral vestibular neurectomy in the adult cat. Eur. J. Neurosci. 25, 47–58. https://doi.org/10.1111/j.1460-9568.2006.05267.x.

Tighilet, B., Leonard, J., Bernard-Demanze, L., Lacour, M., 2015. Comparative analysis of pharmacological treatments with N-acetyl-dl-leucine (tanganil) and its two isomers (N-acetyl-L-leucine and N-acetyl-D-leucine) on vestibular compensation: behavioral investigation in the cat. Eur. J. Pharmacol. 769, 342–349. https://doi.org/10.1016/j.ejphar.2015.11.041.

Tighilet, B., Leonard, J., Lacour, M., 1995. Betahistine dihydrochloride treatment facilitates vestibular compensation in the cat. J. Vestib. Res. 5, 53–66.

Tighilet, B., Léonard, J., Watabe, I., Bernard-Demanze, L., Lacour, M., 2018. Betahistine treatment in a cat model of vestibular pathology: pharmacokinetic and pharmacodynamic approaches. Front. Neurol. 9, 431. https://doi.org/10.3389/fneur.2018.00431.

Tighilet, B., Mourre, C., Trottier, S., Lacour, M., 2007b. Histaminergic ligands improve vestibular compensation in the cat: behavioural, neurochemical and molecular evidence. Eur. J. Pharmacol. 568, 149–163. https://doi.org/10.1016/j.ejphar.2007.04.052.

Tighilet, B., Péricat, D., Frelat, A., Cazals, Y., Rastoldo, G., Boyer, F., Dumas, O., Chabbert, C., 2017. Adjustment of the dynamic weight distribution as a sensitive parameter for diagnosis of postural alteration in a rodent model of vestibular deficit. PLoS One 12, e0187472. https://doi.org/10.1371/journal.pone.0187472.

Tighilet, B., Trico, J., Marouane, E., Zwergal, A., Chabbert, C., 2024. Histaminergic system and vestibular function in normal and pathological conditions. Curr. Neuropharmacol. https://doi.org/10.2174/1570159X22666240319123151.

Tighilet, B., Trottier, S., Lacour, M., 2005. Dose- and duration-dependent effects of betahistine dihydrochloride treatment on histamine turnover in the cat. Eur. J. Pharmacol. 523, 54–63. https://doi.org/10.1016/j.ejphar.2005.09.017.

Tighilet, B., Trottier, S., Mourre, C., Chotard, C., Lacour, M., 2002. Betahistine dihydrochloride interaction with the histaminergic system in the cat: neurochemical and molecular mechanisms. Eur. J. Pharmacol. 446, 63–73. https://doi.org/10.1016/S0014-2999(02)01795-8.

Tighilet, B., Trottier, S., Mourre, C., Lacour, M., 2006. Changes in the histaminergic system during vestibular compensation in the cat. J. Physiol. 573, 723–739. https://doi.org/10.1113/jphysiol.2006.107805.

Van de Heyning, P., Betka, J., Chovanec, M., Devèze, A., Giannuzzi, A.L., Krempaská, S., Przewoźny, T., Scheich, M., Strupp, M., Van Rompaey, V., Meyer, T., 2023. Efficacy and safety of intranasal betahistine in the treatment of surgery-induced acute vestibular syndrome: a double-blind, randomized, placebo-controlled phase 2 study. Otol. Neurotol. 44, 493–501. https://doi.org/10.1097/MAO.0000000000003856.

Wang, J., Liu, B., Xu, Y., Luan, H., Wang, C., Yang, M., Zhao, R., Song, M., Liu, J., Sun, L., You, J., Wang, W., Sun, F., Yan, H., 2022. Thioperamide attenuates neuroinflammation and cognitive impairments in Alzheimer's disease via inhibiting gliosis. Exp. Neurol. 347, 113870. https://doi.org/10.1016/j.expneurol.2021.113870.

Wang, J.-J., Dutia, M.B., 1995. Effects of histamine and betahistine on rat medial vestibular nucleus neurones: possible mechanism of action of anti-histaminergic drugs in vertigo and motion sickness. Exp. Brain Res. 105, 18–24. https://doi.org/10.1007/BF00242178.

Xu, J., Zhang, X., Qian, Q., Wang, Y., Dong, H., Li, N., Qian, Y., Jin, W., 2018. Histamine upregulates the expression of histamine receptors and increases the neuroprotective effect of astrocytes. J. Neuroinflammation 15, 41. https://doi.org/10.1186/s12974-018-1068-x.

Yazdi, A., Doostmohammadi, M., Pourhossein Majarshin, F., Beheshti, S., 2020. Betahistine, prevents kindling, ameliorates the behavioral comorbidities and neurodegeneration induced by pentylenetetrazole. Epilepsy Behav. 105, 106956. https://doi.org/10.1016/j.yebeh.2020.106956.

Zhang, J., Han, X.-H., Li, H.-Z., Zhu, J.-N., Wang, J.-J., 2008. Histamine excites rat lateral vestibular nuclear neurons through activation of post-synaptic H2 receptors. Neurosci. Lett. 448, 15–19. https://doi.org/10.1016/j.neulet.2008.10.027.

Zhang, J., Rong, P., Zhang, L., He, H., Zhou, T., Fan, Y., Mo, L., Zhao, Q., Han, Y., Li, S., Wang, Y., Yan, W., Chen, H., You, Z., 2021. IL4-driven microglia modulate stress resilience through BDNF-Dependent neurogenesis. Sci. Adv. 7, eabb9888. https://doi.org/10.1126/sciadv.abb9888.

Zwergal, A., Günther, L., Brendel, M., Beck, R., Lindner, S., Xiong, G., Eilles, E., Unterrainer, M., Albert, N.L., Becker-Bense, S., Brandt, T., Ziegler, S., la Fougère, C., Dieterich, M., Bartenstein, P., 2017. In vivo imaging of glial activation after unilateral labyrinthectomy in the rat: a [18F]GE180-PET study. Front. Neurol. 8.